

A partially-coupled hydro-mechanical analysis of the Bengal Aquifer System under hydrological loading

Nicholas D. Woodman, William G. Burgess, Kazi Matin Ahmed and Anwar Zahid

Text modifications in response to directions by the Editor

[Please also see Author summary responses to Editor, on the Discussion webpage]

Editor directions are in bold.

Responses are in plain script. Line numbers refer to re-submitted ms showing tracked changes unless otherwise stated.

Added text is given in italics.

1. The authors should highlight the novelty (and the potential impact) of their work

Response: To emphasise the novelty of the paper (also requested by Reviewer#1), the following text has been added to the Introduction at L86:

‘Poro-elastic theory is very well-established, but has not previously been applied in the context of a thick and extensive aquifer such as the BAS to show the implications for groundwater pressures together with solid strains and ground surface displacements.’

Please also note that the four sub-sections of the Discussion each concentrate on a separate aspect of the impact of the research.

2. Section 2.1: Rev 2 suggested to shorten significantly this session, since it does not include any novel element. I tend to agree with Rev 2. In order to facilitate the reading of the manuscript I suggest to move this section to an Appendix (or to include it as supplementary information) - Barometric effects. Add in the manuscript why barometric effects have been neglected (or include them, as suggested by rev 2)

Response: Please see response to point (3) of Reviewer#2. In the re-submitted ms we have made a substantial reduction of Section 2.1 (Poromechanical equations), and have removed the standard derivations to an Appendix, as suggested, thereby replacing L103-137 of the original manuscript by an abbreviated text (not replicated here, but see the tracked-changes ms). Equation references have been renumbered accordingly throughout.

3. check your manuscript carefully for typos, , terminology, updates of data, or updates of variables in equations.

Response: We have made a few typo corrections or minor edits for clarity; please see track-changed ms. This includes some new text inserted at L29 where the following text is added:

“More than 10 million tubewells throughout the basin provide water from BAS for domestic use and for irrigation of the rice crop (Ravenscroft et al., 2009); these include hand-pumped tubewells, normally between 15 and 30 m depth below ground level (bgl), for domestic use, and tubewells installed with motor-driven pumps to abstract water from between 50 and 75 m depth bgl for irrigation of the dry season rice crop (January to April). Municipal water supplies commonly abstract year-round from depths between 200 and 300 m bgl (Shamsudduha et al., 2018).”

Text modifications in response to comments by Reviewer#1

[Please also see responses and rebuttals made as Author responses to Reviewer#1's comments.]

Review comments are in bold.

Responses are in plain script.

Added text is given in italics.

I don't see any new method or development. The only new thing I can see here is just the application, which I think is not enough.

Response: In emphasis of the novelty of the paper (also requested by the Editor), the following text has been added to the to the Introduction at L86 in the re-submitted ms:

'Poro-elastic theory is very well-established, but has not previously been applied in the context of a thick and extensive aquifer such as the BAS to show the implications for groundwater pressures together with solid strains and ground surface displacements.'

Text modifications in response to comments by reviewer#2, Garth van der Kamp

[Please also see responses and rebuttals made as Author responses to Reviewer#2 comments.]

Review comments are in bold.

Responses are in plain script. Line numbers refer to re-submitted ms showing tracked changes unless otherwise stated.

Added text is given in italics.

Specific comments

1. (In the Introduction) ... the phenomenon of groundwater pressure changes due to changes of atmospheric pressure, as expressed through the concept of “barometric efficiency”, is well-known in hydrogeology and is an obvious example of groundwater pressure changes caused by surface loading. It is only mentioned later in the paper (L 199) although it is most directly relevant to the focus of the paper.

Response: In the re-submitted ms, in an addition to the Introduction, we now include the barometric effect as a prime example of surface loading. At L56 the following text is added:

‘Furthermore, it is associated with the well known concept of barometric efficiency (Spane et al., 2002), which describes the response of groundwater pressure to variations in atmospheric pressure, perhaps the example of surface loading effects most familiar to hydrogeologists.’

2. The barometric efficiency of observation wells in deep confined aquifers ... are briefly mentioned in the text (L 186-194) with reference to Burgess et al (2017), but are not further described or used in the paper although they are surely relevant. At the very least a more detailed explanation should be provided of why these results are not used.

Response: In the re-submitted ms, the following text has been added at L251:

‘The discrepancy may alternatively be related to the timescale of processes responsible for changes in groundwater pressure. Barometric efficiency measurements operationally consider short-term pore pressure changes likely corresponding to the response of relatively stiff aquifer sands, whereas pressure changes in clays are expected to become significant in the longer term. Where short-term moisture loading effects are the key interest (Anochikwa et al. 2012, Bardsley and Campbell 2000), values for loading efficiency derived from barometric efficiency may be the most appropriate. Here however our main concern is for poromechanical consistency and for water load changes operating over a range of time scales, therefore we adopt S_s estimates based on field measurements and use the corresponding β and E values (Figure 3).’

3. L102 onwards - Poromechanical equations. This section starts off with a lengthy review of general 3D poro-elastic equations and then arrives back to the 1D differential equation that is used in the subsequent simulations and interpretations. This general review can be largely eliminated from the paper because it does not present anything new that cannot be found in the literature as cited. The paper could then perhaps go directly to the 1D equation (# 9) including the discussion, more or less as given on when and why the 1D equations provide an adequate description of the poro-elastic interactions between stress and groundwater pressure.

Response: In the re-submitted ms we have made a substantial reduction of Section 2.1 (Poromechanical equations), and have removed the standard derivations to an Appendix, as suggested by the Editor, thereby replacing L103-137 of the original manuscript by an abbreviated text (not replicated here, but see the tracked-changes ms). Equation references have been renumbered accordingly throughout.

4. The appropriate equations for the loading efficiency and specific storage should be included - they are not given in the text as it stands.

Response: In the re-submitted ms the equations are given at L168-172.

5. L 148-359. The simulations of the three different loading scenarios can all be considered together as one, by treating the loading effects and the hydraulic head changes at the upper boundary separately. This approach is described and illustrated in detail by Anochikwa et al (2012) a reference that is important for this paper because it presents a somewhat similar analysis of poroelastic effects induced by moisture loading.

Response: Regarding the possible alternative manner of demonstrating the coupled hydro-mechanical effects of surface water loading, individually and collectively in the manner of Anochikwa et al. (2012), in the re-submitted ms we have drawn a comparison between our study and that of Anochikwa et al (2012) in the following text added at L554:

'Anochikwa et al. (2012) assembled field measurements of rainfall and evapotranspiration at a site in Saskatchewan, Canada, using them to define the upper boundary conditions in a one-dimensional model to examine their hydraulic and mechanical loading separately, before summing the outcomes to simulate the overall hydro-mechanical influence on groundwater pressure. Having determined loading efficiency by reference to barometric effects, they then calibrated their 1D model against observed groundwater pressures by varying hydraulic conductivity. At Khulna and Laksmipur, measurements of the separate components of the terrestrial water cycle were not available, hence an indirect demonstration of hydro-mechanical effects was desirable.'

In addition, we have included in the Supporting Information a decomposition analysis such as suggested by Reviewer#2 and in the manner of Anochikwa et al (2012), applied to the field data of groundwater levels at Laksmipur, south-east Bangladesh. We have added the following sentence at L370 of the ms:

'The 'LD' behaviour can be interpreted by means of a decomposition of heads in the manner shown in Anochikwa et al. (2012) (see Supporting Information).'

Further reference to the very relevant paper by Anochikwa et al. (2012) has also been added at lines 72, 199, 255, 619.

6. L 229. Why ignore barometric effects? They can be easily dealt with by direct subtraction from the observation well records, and also provide a good estimate of loading efficiency and compressibility of the formations.

Response: In the re-submitted ms the following sentence is added at L282:

'The daily perturbation on water heads by atmospheric pressure changes is of the order of 0.01m (Burgess et al. 2017), which is small compared to the annual hydrograph amplitude of the order of 1 m. Barometric pressure and earth tides are both neglected for simplicity here.'

Also, in the Discussion section 5.4 of the re-submitted ms, we have added the following sentence at L617:

'Although we omitted barometric effects in the generic simulations for the sake of simplicity, it is straightforward to superpose a further loading signal on top of the existing one if required, as for example when deconvolving deep piezometric signals to make water resources assessments (Anochikwa et al. 2012).'

7. L 260. The assumption that loading efficiency is ~1.0 is questionable and needs more justification, considering that the loading efficiency for barometric loading is an in-situ field measurement that closely corresponds in magnitude to the loading due to changes of TWS. ... This is an important and poorly resolved issue in geolysimetry and merits attention.

Response: Please see response to point 2 above for our justification.

8. L 298-299. The “counter-intuitive” amplitude response to the LD is likely due to a “traveling wave” effect of the transient sinusoidal flows. In fact the flows for this case can be mathematically decomposed as the superposition of the imposed groundwater head changes due to loading (but without flow) and an equal but opposite sinusoidal transient imposed at the water table which induces a downward traveling wave that is dissipated as it moves, but may also be “reflected” from the horizontal boundaries represented by different hydraulic properties, thus giving rise to amplitude and phases that appear anomalous and counter-intuitive.

Response: We agree that decomposition of the solutions is a helpful way to mathematically picture how the apparently anomalous amplitude and phases come about in the ‘load only’ case. In the re-submitted ms we have deleted the words ‘counter intuitive’ at L362, and have added the following sentence at L370:

‘The ‘LD’ behaviour can be interpreted by means of a decomposition of heads in the manner shown in Anochikwa et al. (2012) (see Supporting Information).’

9. LL 337-458 Field data. The reality of the loading effects due to changes of Total Water Storage could likely be demonstrated more strongly by including description and analysis of the short-term loading effects due to individual rain events. Such events are mentioned in the text and appear to be present in the hydrographs shown in figure 6 and especially in figure 7. The sharp spikes with subsequent decay that appear in the rising limbs of the hydrographs are presumably due to large rain events and subsequent runoff and evapotranspiration. Certainly such short-term responses to individual events should be apparent in the hydrographs if the hypothesis of water loading effects is at all correct.

Response: Short-term responses to individual rain events at both field sites are acknowledged (see L386 of the Discussion paper for the Khulna site, “*Episodic deflections on the hydrograph rising limbs, coincident with rainfall events, are likewise simultaneous at all measurement depths*”, and L 431 of the Discussion paper for the Laksmipur site, “*The hydrographs are characterised by a sequence of episodic increments in groundwater head associated with periods of heavy rainfall*”. However, we have not measured other components of the water balance at the sites in the same manner as Anochikwa et al (2012), and therefore cannot deconvolve their individual effects on the groundwater heads. Rather, we have tested the proposition that specific piezometers behave as geological weighing lysimeters (the approach is given at L 349-359 of the Discussion paper), and for this purpose we have applied the appropriate piezometer head record as the upper boundary condition in the model, resolving “*all sources of load acting at the site*”.

10. There is no detailed discussion of the climate of the region and of whether seasonal changes of total water storage of up to 1 meter, as implied by the records for the deep piezometers, are reasonable and realistic.

Response: In the re-submitted ms, the following text has been added at L90:

‘The Bengal Basin has a tropical climate dominated by the Indian monsoon, with annual rainfall increasing from 1500 mm in the south and west to 5500 mm in north-east Bangladesh, of which 85% falls during the summer rainy season (May to November) when individual storm events can

contribute over 100 mm per day (Ravenscroft, 2003). During the monsoon season, river levels rise by 2-8 m leading to widespread flooding (Steckler et al., 2010) with up to 30% of the land surface routinely being flooded to a depth up to ca. one metre. During the Boro rice irrigation season (January to April), groundwater pumping for irrigation throughout rural areas commonly provides standing water across rice paddies to a depth of ca 0.1 m (Hasanuzzaman, 2003).'

11. L 449 the speculative uncertainty with regard to loading efficiency could perhaps be resolved by inspection of the responses at each depth to episodic rainfall events. As mentioned previously a description and analysis of barometric loading effects for the same piezometers would further establish the reality of the poroelastic responses to changes of total water storage.

Response: Please see Responses to points 9 and 2.

Technical corrections

The reference information for Burgess et al (2017) is incomplete and requires more information

Response: The publication details are now complete.

LL 110-115 Can't have some units as Pa and others as MPa. That would require introduction of factors of 10^6 in the equations.

Response: We confirm that identical units were included in application of equation (1) so no corrections to our working are needed.

A partially-coupled hydro-mechanical analysis of the Bengal Aquifer System under hydrological loading

Nicholas D. Woodman^{1†}, William G. Burgess¹, Kazi Matin Ahmed² and Anwar Zahid³

¹Department of Earth Sciences, University College London, London WC1E 6BT, UK, ²Department of Geology, Dhaka University, Dhaka 1000, Bangladesh, ³Bangladesh Water Development Board, Dhaka, Bangladesh, [†]current address: Faculty of Engineering and the Environment, University of Southampton, Southampton SO17 1BJ, UK

Correspondence to: Nicholas D Woodman (n.d.woodman@soton.ac.uk)

Abstract. The coupled poro-mechanical behaviour of geologic-fluid systems is fundamental to numerous processes in structural geology, seismology and geotechnics but is frequently overlooked in hydrogeology. Substantial poro-mechanical influences on groundwater head have recently been highlighted in the Bengal Aquifer System, however, driven by terrestrial water loading across the Ganges-Brahmaputra-Meghna floodplains. Groundwater management in this strategically important fluvio-deltaic aquifer, the largest in south Asia, requires a coupled hydro-mechanical approach which acknowledges poro-elasticity. We present a simple partially-coupled, one-dimensional poro-elastic model of the Bengal Aquifer System, and explore the poro-mechanical responses of the aquifer to surface boundary conditions representing hydraulic head and mechanical load under three modes of terrestrial water variation. The characteristic responses, shown as amplitude and phase of hydraulic head in depth profile and of ground surface deflection, demonstrate (i) the limits to using water levels in piezometers to indicate groundwater recharge, as conventionally applied in groundwater resources management; (ii) the conditions under which piezometer water levels respond primarily to changes in the mass of terrestrial water storage, as applied in geological weighing lysimetry; (iii) the relationship of ground surface vertical deflection to changes in groundwater storage; and (iv) errors of attribution that could result from ignoring the poroelastic behaviour of the aquifer. These concepts are illustrated through application of the partially-coupled model to interpret multi-level piezometer data at two sites in southern Bangladesh. There is a need for further research into the coupled responses of the aquifer due to more complex forms of surface loading, particularly from rivers.

1 Introduction

Throughout the Bengal Basin, the floodplains of the Ganges, Brahmaputra and Meghna (GBM) rivers (Fig. 1) are underlain by the Bengal Aquifer System (BAS), the largest aquifer in south Asia and the source of water to over 100 million people (Burgess et al., 2010). [More than 10 million tubewells throughout the basin provide water from BAS for domestic use and for](#)

30 [irrigation of the rice crop](#) (Ravenscroft et al., 2009); [these include hand-pumped tubewells, normally between 15 and 30 m](#)
31 [depth below ground level \(bgl\), for domestic use, and tubewells installed with motor-driven pumps to abstract water from](#)
32 [between 50 and 75 m depth bgl for irrigation of the dry season rice crop \(January to April\). Municipal water supplies commonly](#)
33 [abstract year-round from depths between 200 and 300 m bgl](#) (Shamsudduha et al., 2018). Management of the BAS groundwater
34 resource relies on monitoring water levels in networks of observation boreholes, taking the conventional approach that changes
35 in groundwater heads represent volumetric changes in groundwater storage through recharge and drainage (Shamsudduha et
36 al., 2011). This approach presumes the hydraulic behaviour of the aquifer to be decoupled from its mechanical response to
37 changes in stress. Recently, however, the distinctively poroelastic behaviour of the BAS has been recognised (Burgess et al.,
38 2017), by which groundwater heads are subject to substantial mechanical perturbation driven by changes in the mass of
39 terrestrial water storage (TWS) above the surface of the aquifer. A coupled hydro-mechanical approach is necessary for
40 understanding groundwater conditions and managing resources in this environment, particularly in relation to recharge
41 (Shamsudduha et al., 2012), sustainability of groundwater abstraction for irrigation (Shamsudduha et al., 2008) and municipal
42 water supply (Ravenscroft et al., 2013), and the security of schemes for mitigation against groundwater arsenic (Michael and
43 Voss, 2008) and salinity (Rahman et al., 2011; Sultana et al., 2015).

44
45 The generally coupled poro-mechanical nature of geologic-fluid systems is well-established (Neuzil, 2003); porewater
46 pressures affect the stress state and vice-versa. These interactions are accepted as important where groundwater conditions are
47 related to faulting (Roeloffs, 1988; Rojstaczer and Agnew, 1989; Sutherland et al., 2017), earthquakes (Manga et al., 2012),
48 pumping-induced aquitard responses (Verruijt, 1969), ground subsidence (Burbey et al., 2006; Erban et al., 2014), glacial
49 loading effects (Bense and Person, 2008; Black and Barker, 2016) and surface water interactions (Acworth et al., 2015; Boutt,
50 2010). Use of ground surface vertical displacements to infer aquifer or groundwater conditions (Chaussard et al., 2014; Reeves
51 et al., 2014) is also predicated on coupling of the hydraulic and mechanical behaviour of aquifer sediments. For simulation of
52 transient groundwater flow in aquifers, however, a decoupling simplification is frequently applied such that the elastic equation
53 does not need to be solved simultaneously. Thus, the flow equation is solved without consideration of internal stresses and
54 strains or mechanical boundary conditions. Despite this, the poro-mechanical nature of confined aquifers is embedded in the
55 concept of specific storage which incorporates the elastic compressibility of the aquifer materials (Domenico and Schwartz,
56 1998; Green and Wang, 1990; Narasimhan, 2006). [Furthermore, it is associated with the well known concept of barometric](#)
57 [efficiency](#) (Spane, 2002), [which describes the response of groundwater pressure to variations in atmospheric pressure, perhaps](#)
58 [the example of surface loading effects most familiar to hydrogeologists](#). The decoupling assumption is reasonable where the
59 effects of mechanical loading can be considered insignificant, either when the changes in load are small, or when the applied
60 load is mostly borne by the solid rather than the fluid (Black and Barker, 2016). Neither of these conditions apply to the BAS
61 sediments, which are highly compressible (Steckler et al., 2010) and subject to substantial and extensive TWS mechanical
62 loads due to heavy rainfall, deep flooding and large river discharges as a consequence of the annual monsoon (Shamsudduha
63 et al., 2012).

65 In the event of laterally-extensive changes to mechanical loads and/or hydraulic heads above the surface of an aquifer, and
 66 laterally-homogeneous aquifer properties, by symmetry it may be deduced that lateral strains are zero. This condition gives
 67 rise to a *partial* coupling of the elastic and fluid pressure equations (Neuzil, 2003). In the case of *partial* coupling, changes to
 68 the mechanical load due to the changing mass of water near or at the surface may be included within the flow equation, one-
 69 dimensionally in the vertical direction, and the solutions will satisfy all the equilibrium and compatibility requirements for
 70 stress and strain. There is no need to solve the elastic equation in order to calculate pressures in the aquifer, although once the
 71 flow equation is solved, the pressures can be substituted into the elastic equation to provide stresses and strains (Anochikwa
 72 et al., 2012). A sub-set of this partially-coupled condition occurs where there is negligible groundwater flow, due to very low
 73 hydraulic gradients, low permeability or a combination of both. This can be the situation in extensive fluvio-deltaic aquifers
 74 of low topographic relief such as the BAS (Burgess et al., 2017) if mechanical loading is imposed at the surface in a manner
 75 which does not induce significant vertical hydraulic gradients. Under these conditions, porewater pressures are determined by
 76 changes to surface mechanical loading alone, and changes in groundwater head may be taken as a measure of changes in TWS
 77 mechanical loading above the surface of the aquifer. This is the conceptual basis for geological weighing lysimetry (van der
 78 Kamp and Schmidt, 1997; Bardsley and Campbell, 1994, 2007; van der Kamp and Schmidt, 2017) as used in diverse
 79 environments to determine Δ TWS at the scale of individual catchments (Marin et al., 2010; Lambert et al., 2013; Barr et al.,
 80 2000; Smith et al., 2017). Geological weighing lysimetry has been suggested as suitable for mapping the variability of Δ TWS
 81 within the Bengal Basin (Burgess et al., 2017; Bardsley and Campbell, 2000), complementary to basin-scale estimates based
 82 on the Gravity and Climate Recovery Experiment (GRACE) satellite mission (Tapley et al., 2004; Tiwari et al.,
 83 2009; Shamsudduha et al., 2012).

84

85 The purpose of this paper is to explore the behaviour of the BAS as a poroelastic aquifer subject to a variety of extensive TWS
 86 mechanical and hydraulic loads. Poro-elastic theory is very well-established, but has not previously been applied in the
 87 context of a thick and extensive aquifer such as the BAS to show the implications for groundwater pressures together with
 88 solid strains and ground surface displacements.

89

90 The Bengal Basin has a tropical climate dominated by the Indian monsoon, with annual rainfall increasing from 1500 mm in
 91 the south and west to 5500 mm in north-east Bangladesh, of which 85% falls during the summer rainy season (May to
 92 November) when individual storm events can contribute over 100 mm per day (Ravenscroft, 2003). During the monsoon
 93 season, river levels rise by 2-8 m leading to widespread flooding (Steckler et al., 2010) with up to 30% of the land surface
 94 routinely being flooded to a depth up to ca. one metre. During the Boro rice irrigation season (January to April), groundwater
 95 pumping for irrigation throughout rural areas commonly provides standing water across rice paddies to a depth of ca 0.1 m
 96 (Hasanuzzaman, 2003). For the purpose of this paper, we treat the separate components of TWS across the GBM floodplains
 97 as inundation (free-standing surface water such as paddy, floods, beels, and ponds), unconfined storage (water in the

98 unsaturated zone and in saturated pores in the intermittently saturated zone of the aquifer), *elastic storage* (water in the
99 saturated pores in the permanently saturated zone), and *rivers* (surface water flowing in rivers and drainage channels).
100 Processes that alter the TWS loads include rainfall and evaporation, rising and falling river stage, flooding and drainage of the
101 land surface, varying soil moisture storage and a fluctuating water table. Groundwater pumping modifies the water balance
102 and induces additional hydro-mechanical responses. These processes differ in their timing, the geometry of the TWS stores
103 they affect and the relationship between their resultant hydraulic and mechanical expressions. First, we apply the concept of
104 *partial* coupling to seek characteristic responses of the aquifer to extensive TWS loads originating as (a) surface water
105 inundation, (b) water table fluctuation and (c) water bodies hydraulically isolated from the aquifer. These loading styles are
106 examined with and without pumping. The results address important questions for the BAS which are likely also relevant to
107 similarly extensive and strategically important fluvio-deltaic aquifer systems elsewhere in south Asia (Fendorf et al.,
108 2010; Benner et al., 2008; Larsen et al., 2008; Tam et al., 2014; Xu et al., 2011): how can piezometer heads in the poroelastic
109 aquifer be used to indicate recharge, as required for conventional groundwater resources management; under what conditions
110 can piezometer heads be used to measure Δ TWS using geological weighing lysimetry; can ground surface deflections be related
111 to changes in groundwater storage; and what errors may arise if the poroelastic behaviour of the aquifer is ignored? Second,
112 we apply the partial coupling approach to these questions in the BAS, with reference to multi-level piezometer data from
113 Khulna and Laksmipur in southern Bangladesh (Fig. 1).

114 **2 Methods**

115 We firstly set out the partially-coupled 1D poromechanical approach that we use to examine the implications of specific surface
116 (upper boundary) loading scenarios, with aquifer parameters set to represent the BAS underlying the GBM floodplains (Fig.
117 1). We consider an equivalent homogeneous uniform medium, as well as a layered structure based on lithological sections.
118 The results provide a diagnostic framework which we apply to analysis of loading styles at Khulna and Laksmipur in southern
119 Bangladesh.

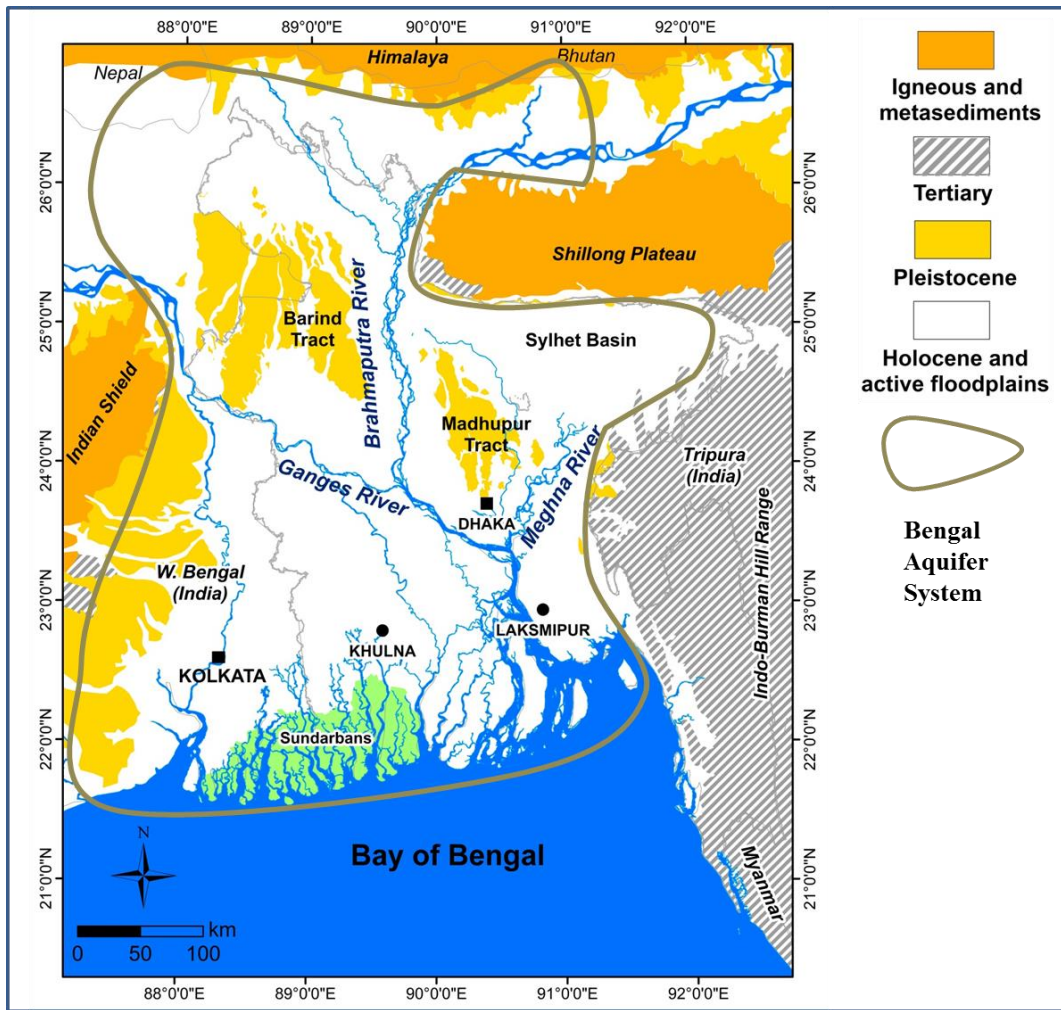


Figure 1. Location map showing the extent of the Bengal Aquifer System (BAS) and the Ganges-Brahmaputra-Meghna (GBM) floodplains.

2.1 Poromechanical equations

We concentrate on the isothermal coupling between water flow and the elastic behaviour of the BAS sediment, and assume that the aquifer material behaves in a linear elastic way. This is likely to be reasonable under repeated mechanical load-unload cycles, provided there is no secular decline in groundwater level sufficient to cause effective stress to exceed the previous loading maximum.

The governing equations for elastic deformation of a porous solid can be derived from the constitutive equations for stress, force equilibrium and strain compatibility. In 3D, the poro-elastic constitutive relations between elastic stress and strain are the same as the classical relationships for an elastic solid coupled to the pore pressure by Terzaghi's effective stress law (Neuzil, 2003):

$$\sigma_{ij} = 2G \epsilon_{ij} + 2G \frac{\nu}{1-2\nu} \epsilon_{kk} \delta_{ij} + \alpha_B p \delta_{ij} \quad (1)$$

where, δ_{ij} is the Kronecker delta (which is zero when $i \neq j$ and one when $i = j$) and following the Einstein Summation convention; stresses (σ_{ij}) and strains (ϵ_{ij}) are positive in compression; p is the porewater pressure (Pa), ν is Poisson's ratio (-), G is the shear modulus (MPa), and $\alpha_B = 1 - K/K_s$, where, K (MPa) is the bulk modulus of the porous medium and K_s (MPa) is the bulk modulus of the solid grains. Here we assume that the solid grains are effectively incompressible ($K_s \gg K$) and hence $\alpha_B = 1$.

Equation (1) can be simplified to 1D where there is a uniform mechanical load with wide lateral extent such that there are no lateral strains. The medium is considered to sit on a rigid base, with the top surface free to move, so strain can only be vertical, thus:

$$\sigma_{zz} = K' \epsilon_{zz} + \alpha_B p \quad (2)$$

where,

$$K' = 3K(1-\nu)/(1+\nu) \quad (3)$$

and the bulk modulus, K and shear modulus, G are related to Young's modulus E by $K = \frac{E}{3(1-2\nu)}$ and $G = \frac{E}{2(1+\nu)}$. Just as the elastic equations have a pore pressure term, the isothermal, Darcian groundwater flow equation contains a coupled stress term (Neuzil, 2003):

$$\nabla \cdot \kappa (\nabla p + \rho g \nabla z) = S_{ss} \frac{\partial p}{\partial t} - S_{ss} \beta \frac{\partial \sigma_e}{\partial t} - gJ \quad (4)$$

where κ is the hydraulic conductivity (m s^{-1}), p is the pore pressure (Pa), z is the elevation (m), J is a source term used here to simulate groundwater abstraction by pumping and $\sigma_e = (\sigma_{xx} + \sigma_{yy} + \sigma_{zz})/3$ (Pa).

Changes to σ_e (here termed 'mechanical loads') are applied as a boundary condition at the surface, and are transmitted by the solid skeleton to the entire solid at the acoustic velocity. This represents partial 'coupling'; if there are no internal loads applied and provided the changes to the surface load are known, then the flow equation can be solved without a need to solve the elastic equations. Deformations can be found from Eq. (2), in conjunction with the compatibility relationships.

The 3D specific storage is defined as:

$$S_{ss} = \rho g \left[\left(\frac{1}{K} - \frac{1}{K_s} \right) + \left(\frac{n}{K_f} - \frac{n}{K_s} \right) \right] \quad (5)$$

where n is the porosity, and K_f is the modulus of the water (MPa). The (3D) loading efficiency, or Skempton's coefficient, β , is defined as:

$$\beta = \frac{\left(\frac{1}{K} - \frac{1}{K_s} \right)}{\left(\frac{1}{K} - \frac{1}{K_s} \right) + \left(\frac{n}{K_f} - \frac{n}{K_s} \right)} \quad (6)$$

In the event of uniform areal mechanical loading, and where lateral strains are negligible, Eq. (4) simplifies to 1D:

$$\nabla \cdot \frac{\kappa \rho g}{\mu} (\nabla p + \rho g \nabla z) = S_s \frac{\partial p}{\partial t} - S_s \xi \frac{\partial \sigma_{zz}}{\partial t} - gJ \quad (7)$$

where $\xi = \beta(1 + \nu)/[3(1 - \nu) - 2\alpha\beta(1 - 2\nu)]$ is the one-dimensional loading efficiency and S_s is the one-dimensional specific storage (van der Kamp and Gale, 1983)

$$S_s = S_{s3}(1 - \lambda\beta) \quad (8)$$

where $\lambda = 2\alpha_B(1 - 2\nu)/3(1 - \nu)$.

We therefore consider a simplified system: a 1D column of aquifer with no flow boundaries on the sides and base, and no horizontal strain (Fig. 2).

We concentrate on the coupling between water flow and the mechanical behaviour of the BAS sediment, assuming isothermal conditions and that the aquifer material behaves in a linear-elastic way. This is likely to be reasonable under repeated mechanical load-unload cycles, provided there is no secular decline in groundwater level sufficient to cause effective stress to exceed the previous loading maximum.

The 3D flow and mechanical equations are given in the Appendix. In the event of uniform areal mechanical loading, and where lateral strains are negligible, the system simplifies to a 1D flow equation coupled to a mechanical equation. The 1D flow equation is:

$$\nabla \cdot \kappa (\nabla p + \rho g \nabla z) = S_s \frac{\partial p}{\partial t} - S_s \xi \frac{\partial \sigma_{zz}}{\partial t} - gJ \quad (1)$$

where κ is the hydraulic conductivity (m s^{-1}), ρ is the fluid density (kg m^{-3}), p is the pore pressure (Pa), z is the elevation (m), J ($\text{kg m}^{-3}\text{d}^{-1}$) is a fluid source term used here to simulate groundwater abstraction by pumping. The one-dimensional loading efficiency is given by $\xi = \beta(1 + \nu)/[3(1 - \nu) - 2\alpha_B\beta(1 - 2\nu)]$, ν is Poisson's ratio (-), α_B is the Biot-Willis coefficient (assumed equal to 1 to simulate incompressible particle grains) and β is the 3D loading efficiency given in the Appendix (A4). $S_s = S_{s3}(1 - \lambda\beta)$ is the one-dimensional specific storage (van der Kamp and Gale, 1983), where $\lambda = 2\alpha_B(1 - 2\nu)/3(1 - \nu)$ and S_{s3} is given in the Appendix (A3).

The sediment is assumed to sit on a rigid base, with the top surface free to move, so strain can only be vertical. Thus from Equation A1, the vertical stress and strains are related by:

$$\sigma_{zz} = K' \varepsilon_{zz} + \alpha_B p \quad (2)$$

where $K' = 3K(1 - \nu)/(1 + \nu)$ and the bulk modulus, K and shear modulus, G are related to Young's modulus E by $K = \frac{E}{3(1 - 2\nu)}$ and $G = \frac{E}{2(1 + \nu)}$. Changes to the total vertical stress, σ_{zz} (here termed 'mechanical loads') are applied as a boundary condition at the surface, and are transmitted by the solid skeleton to the entire solid at the acoustic velocity. This represents

'partial coupling'; if there are negligible internal loads and provided the changes to the surface load are known, then the flow equation (1) can be solved without a need to solve the elastic equations. Deformations can be found from Eq. (2), in conjunction with the compatibility relationships.

The simplified system considered here is given in Fig. 2. On the upper boundary, the changing TWS is simulated by means of a changing head and a changing mechanical load, according to the nature of the contributing hydrological components. Under this simplification, vertical displacement at the surface will arise in only two ways: by contraction or expansion of the pore space where there is a net change in the volume of water in the column, and by contraction or expansion of the pore water. Being limited to 1D movement, these volume changes are entirely taken up by vertical displacement.

The reference frame is the base of the model which is assumed fixed in space and set at 1 km depth, acknowledging the variation in aquifer thickness between south-east Bangladesh, 3000 m (Michael and Voss, 2009a) and West Bengal, 300 m (Mukherjee et al., 2007). Within this domain, equations (1) & (2) are solved analytically for a homogeneous uniform material in the absence of pumping, and numerically where layers of individually homogeneous materials are simulated, with and without pumping. Where pumping is simulated, the water is assumed to be taken uniformly from the pumping-interval. For simplicity, earth-tides are neglected.

2.2 Analytical solution

Taking Eq. (1) and assuming homogeneous K , E and that $J = 0$, converting p to metres head, h (i.e. $h = \rho g p + z$), and σ_{zz} to metres of load (i.e. $L = \sigma_t / \rho g$, where ρ (kg m⁻³) is the density of water and g (m s⁻²) is the acceleration due to gravity) (Anochikwa et al., 2012; van der Kamp and Schmidt, 1997) gives:

$$D \frac{\partial^2 h}{\partial z^2} = \frac{\partial h}{\partial t} - \xi \frac{\partial L}{\partial t} \quad (93)$$

where 1D hydraulic diffusivity is defined as $D = \frac{k \rho g}{\mu S_s}$.

Applying the following sinusoidal hydraulic and mechanical loading boundary conditions to Eq. (9) where we introduce parameter, α , which can be set to zero to give the case of a load in the absence of a varying head, and otherwise is kept at 1:

$$h(0, t) = H(t) = \alpha H_0 \cos(\omega t) \quad (104)$$

$$L(t) = S_y H_0 \cos(\omega t)$$

The following solution is obtained:

$$h(z, t) = \alpha B \cos(\omega t - \psi) \quad (115)$$

where ψ is the lag (in radians) behind the head $H(t)$ and mechanical loads $L(t)$ at the boundary and:

$$B = \sqrt{\gamma^2 + 2\gamma(\alpha - \gamma)e^{-\theta} \cos(\theta) + (\alpha - \gamma)^2 e^{-2\theta}} \quad (126)$$

$$\psi = \tan^{-1} \left(\frac{(\alpha - \gamma) \sin(\theta)}{(\alpha - \gamma) \cos(\theta) + \gamma e^{\theta}} \right)$$

$$\theta = z \sqrt{\frac{\omega}{2D}} = z \sqrt{\frac{\pi}{DT}} \quad \text{and} \quad \gamma = S_y \xi$$

205 In the event that the mechanical load, L , is negligible compared to applied head H (e.g. where either S_y is very small
206 or ξ is very small), the hydraulic-only solution is well known (van der Kamp and Maathuis, 1991):

$$h(z, t) = H_0 \exp(-\psi) \cos(\omega t - \psi) \quad (137)$$

207 where the lag is now $\psi = \theta$. Thus, the lag increases with depth or with increasing forcing frequency and the amplitude
208 decreases exponentially with θ .

209 Displacement and change in groundwater storage can be calculated as the time integral of velocity at the surface. Applying
210 Darcy's law at the surface ($z=0$) and integrating gives:

$$u = \Delta S = \int_0^t K \left. \frac{dh}{dz} \right|_{z=0} dt' \quad (148)$$

211 Equation (148) can be computed by differentiating Eq. (145) w.r.t. z and then numerically integrating over time. Alternatively,
212 the change of storage can be reported from the numerical model.

213 2.3 Numerical solution

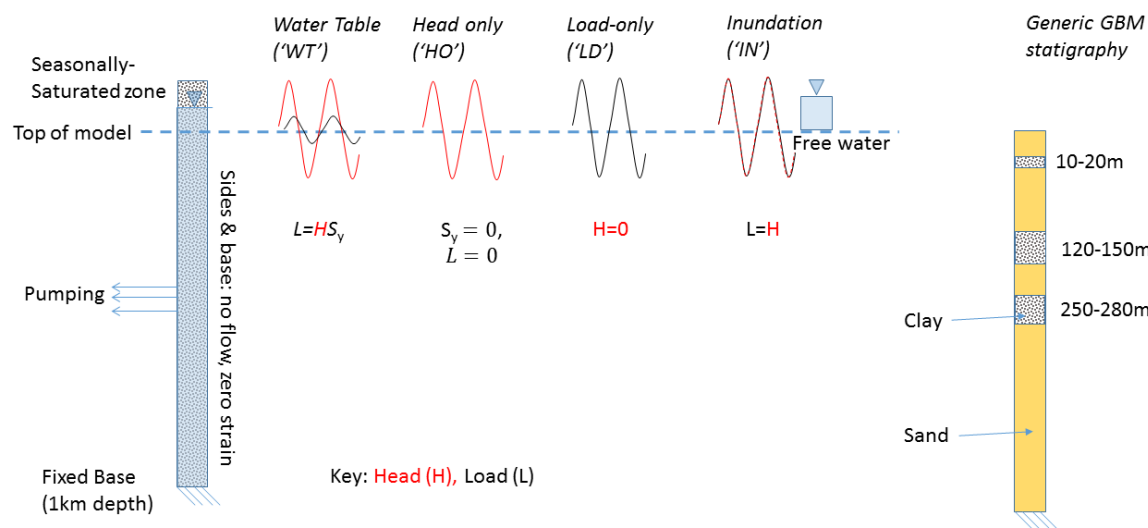
214 We used the COMSOL Multiphysics® software, validated against the analytical solutions for uniform permeability, to solve
215 the stress and flow equations (1) and (42). The finite-element model is unrestricted in terms of spatial distribution of parameter
216 properties and in terms of the boundary condition functions.

217 2.4 Parameter allocation

218 Selected parameter values for the BAS underlying the GBM floodplains are given in Fig. 2. The bulk values for the uniform
219 representations are close to the harmonic average of the series components. We next discuss the context in which these
220 parameter selections are made.

221 2.4.1 Modulus of elasticity, storativity and loading efficiency

222 Text-book S_s values (Domenico and Schwartz, 1998) for the materials in the Bengal Basin range between approximately 1×10^{-5}
223 m^{-1} (dense sandy gravel) and $1 \times 10^{-2} \text{m}^{-1}$ (plastic clay). In large-scale modelling of head recession data in the basin Michael
224 & Voss (Michael and Voss, 2009b) achieved their best fits when S_s was $9.4 \times 10^{-5} \text{m}^{-1}$ taking pumped abstraction to be areally
225 uniform. This is the basis for the range in specific storage, S_s , for the BAS (Fig. 2).



	Uniform <i>homogeneous</i>	Layered representation						
		1 (sand)	2 (silty-clay)	3 (sand)	4 (silty-clay)	5 (sand)	6 (silty-clay)	7 (sand)
Thickness (m)	1000	10	10	100	30	100	30	720
S_y (-)	0.1 ¹	0.1	-	-	-	-	-	-
S_s (m ⁻¹)	0.00001 ²	1×10^{-5}	1×10^{-4}	1×10^{-5}	1×10^{-4}	1×10^{-5}	1×10^{-4}	1×10^{-5}
K_v (ms ⁻¹)	0.00000005 ³	1×10^{-5}	1×10^{-8}	1×10^{-5}	1×10^{-8}	1×10^{-5}	1×10^{-8}	1×10^{-5}
E (MPa)	82.07	850.89	82.07	850.89	82.07	850.89	82.07	850.89
β (-)	0.996	0.961	0.996	0.961	0.996	0.961	0.996	0.961
ξ (-)	0.993	0.932	0.993	0.932	0.993	0.932	0.993	0.932

Figure 2. The 1D model showing (top) the upper surface boundary conditions with head as red lines and mechanical load (weight) as black lines, expressed as metres of water; and a representative stratigraphy for the BAS underlying the GBM floodplains, with the profile depth being 1 km; and (bottom) parameter values for the uniform and layered 1D representations. Porosity is taken as 0.1 throughout; $\nu=0.25$; E , β and ξ are calculated using Equations (5A3) and (6A4). ¹ (Shamsudduha et al., 2011); ² (Burgess et al., 2017); ³ (Michael and Voss, 2009a).

Specific storage S_s and Young's Modulus E are related through Eq. [5A3] and to the loading efficiency β via Eq. (6A4). These inter-relationships are plotted in Fig. 3. It is notable that for $E < 1$ GPa, $\beta > 0.95$ and $S_s > 1 \times 10^{-5} \text{ m}^{-1}$. Thus the loading efficiency only falls significantly below 1 for materials stiffer than around 1 GPa, and where the specific storage is less than $1 \times 10^{-5} \text{ m}^{-1}$. Uncemented sediment is thus expected to have $\beta \sim 1$ (Bakker, 2016); on this basis the BAS sediment is unlikely to be sufficiently stiff in the top few hundred metres to allow decoupling of the stress and flow equations. This is confirmed by in situ, high-pressure dilatometer measurements (de Silva et al., 2010) giving E within the broad range for sediments given in Fig. 3.

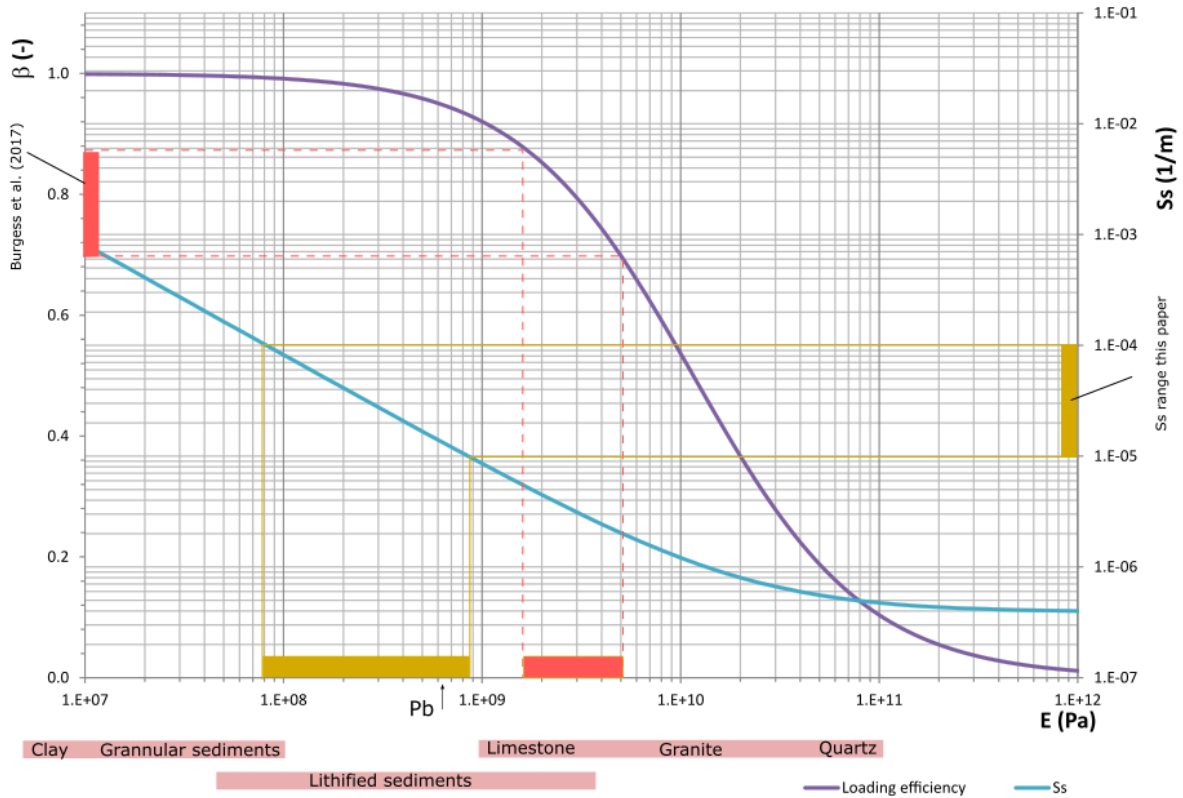


Figure 3. Relationship between 1D Specific storage (S_s), Young's modulus (E) and 3D loading efficiency (β) using equations (5A3) and (6A4) assuming porosity of 0.1 and Poisson's ratio of 0.25. Projections show the corresponding inferred ranges of E based on the S_s range applied ($1 \times 10^{-5} - 1 \times 10^{-4} \text{ m}^{-1}$) and the loading efficiencies calculated via barometric efficiency estimates (0.69-0.87) by Burgess et al. 2017. Pink bars show indicative ranges for common geological materials. Arrow indicates data from 73 m depth at Padma Bridge (Pb) (De Silva et al., 2010).

Estimates of loading efficiency based (Jacob, 1940) on barometric efficiency are rather lower: a range of 0.69-0.87 has been determined at Laksmipur in the GBM sediment (Burgess et al., 2017). This is potentially indicative of a considerable stiffening due to burial (E in the range 6-17 GPa), indicating S_s in the range 1×10^{-6} to $9 \times 10^{-8} \text{ m}^{-1}$. Such a condition might be expected in a Gibson soil (Gibson, 1974; Powrie, 2014). However, the Laksmipur estimates do not decrease systematically with depth,

possibly due to changes in stiffness in different materials. [The discrepancy may alternatively be related to the timescale of processes responsible for changes in groundwater pressure. Barometric efficiency measurements operationally consider short-term pore pressure changes likely corresponding to the response of relatively stiff aquifer sands, whereas pressure changes in clays are expected to become significant in the longer term. Where short-term moisture loading effects are the key interest](#) (Anochikwa et al., 2012; Bardsley and Campbell, 2000), [values for loading efficiency derived from barometric efficiency may be the most appropriate. Here however our main concern is for poromechanical consistency and for water load changes operating over a range of time scales. Therefore](#) ~~therefore for the purposes of this paper~~ we adopt S_s estimates based on field measurements and use the corresponding β and E values ([Figure 3](#)).

2.4.2 Hydraulic conductivity

Basin scale modelling suggests a horizontal-vertical anisotropy for hydraulic conductivity in the BAS of $\sim 10,000$ (Michael and Voss, 2009b; Ravenscroft et al., 2005). This may be explained as an effective, large-scale value incorporating finer-scale detail of the highly heterogeneous sedimentary record of the past deltaic environment where low permeability lenses and drapes are laterally discontinuous (Hoque et al., 2017). (Michael and Voss, 2009a) cite aquifer tests (Hussain and Abdullah, 2001) conducted by the Bangladesh Water Development Board (BWDB) giving a range for hydraulic conductivity (κ) from 3×10^{-5} to $1 \times 10^{-3} \text{ m s}^{-1}$. Accounting for anisotropy, κ_v may therefore locally be in the range $\sim 1 \times 10^{-9}$ to $1 \times 10^{-7} \text{ m s}^{-1}$. The κ_v values of the uniform and layered representations of the BAS underlying the GBM floodplains (Fig. 2) and of silty-clay in layered representations of the Khulna and Laksmipur sites (Sect. 4) lie within this range.

2.4.3 Specific yield

Specific yield is the drainable porosity of the material in which the water table moves. (Michael and Voss, 2009b) cite a range from 0.02 to 0.19 in Bangladesh, noting that much of the Basin has a specific yield in the range of 0.02–0.05. We take $S_y=0.1$ and 0.01 as order-of-magnitude values typical for sand and clay respectively (Domenico and Schwartz, 1998).

2.5 Upper boundary conditions and groundwater abstraction

Changes to the shallow water budget which have the potential to be laterally-extensive and uniform include: water arriving as rainfall at the surface and either ponding or moving to the shallow water table as recharge; and water departing the surface or the water table by evaporation, or as runoff to the extensive network of drainage channels. Pumping for domestic and irrigation supply may potentially be considered as areally-uniform, where sufficiently common and over a wide area (Michael and Voss, 2008). The changing shallow water budget causes a change in mechanical loading to the aquifer system, and if in direct hydraulic continuity with the saturated water column it also causes a change in head. If the shallow water is not hydraulically connected to the saturated aquifer system, the effects of the changing water budget are transmitted to depth by mechanical compression/extension of the sediment, but not by hydraulic diffusion. Changes to the barometric pressure also apply a laterally-extensive changing force to the surface of the aquifer and to the water column, and earth tides are also laterally-

extensive. [The daily perturbation on water heads by atmospheric pressure changes is of the order of 0.01m](#) (Burgess et al., 2017), [which is small compared to the annual hydrograph amplitude of the order of 1 m. Barometric pressure and earth tides are Both both effects are](#) neglected for simplicity here.

To explore the consequences of these hydraulic and mechanical loading sources, the groundwater dynamics associated with three upper surface boundary conditions are modelled here (Fig. 2). Firstly, the effect of a changing level of free water is examined, such as would be seen in paddy-fields, ponds or during floodwater inundation. This condition is here termed ‘IN’. The change in free-water level is equal to both the change in head and the change in mechanical load at the upper surface (load is here parameterised in metres of water rather than as a stress). Secondly, the effect of changes to unconfined storage due to a moving water table is examined. This condition is here termed ‘WT’. The change in load is the specific yield times the head. For very small specific yields this condition approaches the hydraulic-only (‘HO’) loading case, whereby there is insignificant mechanical load, despite the change in head. Thirdly, we examine the effect of a changing surface water store (which could be either free water held above an impermeable barrier, or a perched phreatic aquifer) which is hydraulically isolated from the main aquifer system. A mechanical load only is applied, therefore no head change is applied to the aquifer and this condition is termed ‘LD’.

These three TWS loading scenarios are applied in turn to a uniform and a layered representation of the BAS underlying the GBM floodplains. The loading is applied as sinusoidal functions with unit amplitude and time period of 1 year to simulate the annual hydrological cycle. Additionally, the effects of groundwater abstraction are simulated. Abstraction is taken evenly from the depth interval 50-100 m at an average rate of 0.2 m a^{-1} , either as continuous pumping or as discontinuous pumping π out of phase with the TWS load, as a coarse representation of seasonally-varying pumping for irrigation during the dry season.

3 Forward modelling results

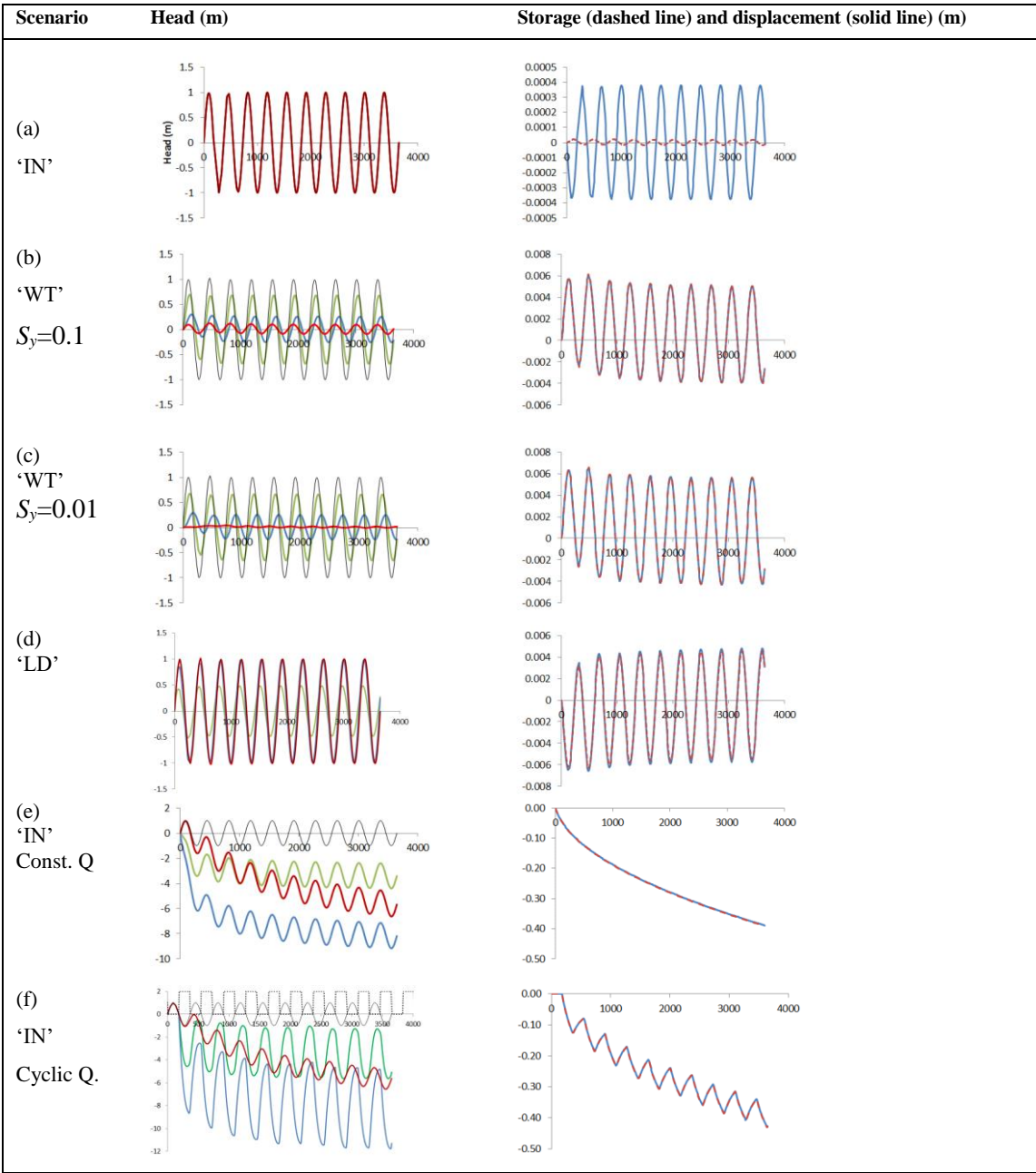
The modelled responses of groundwater head to sinusoidal hydraulic and mechanical source terms, together with changes in groundwater storage and ground surface vertical displacements, are illustrated for the GBM environment with uniform properties in Figures 4 and 5. Figure 4 shows the modelled responses over ten years at depths of 30, 100 and 300 m, approximating typical BWDB multi-level piezometers (BWDB, 2013). The depth variations of amplitude and phase for groundwater head and the phase-lag for surface displacement are summarised in Fig. 5. The effect of layering (Supporting Information) is to cause departure from the uniform cases, so interpretation of data in a real, heterogeneous aquifer should take into account local deviation from idealised uniform conditions. However, in general, the loading style (‘IN’, ‘WT’, ‘LD’) and

312 pumping regime are of more significance for the head responses and surface displacements than the detail of the BAS
313 stratigraphy.

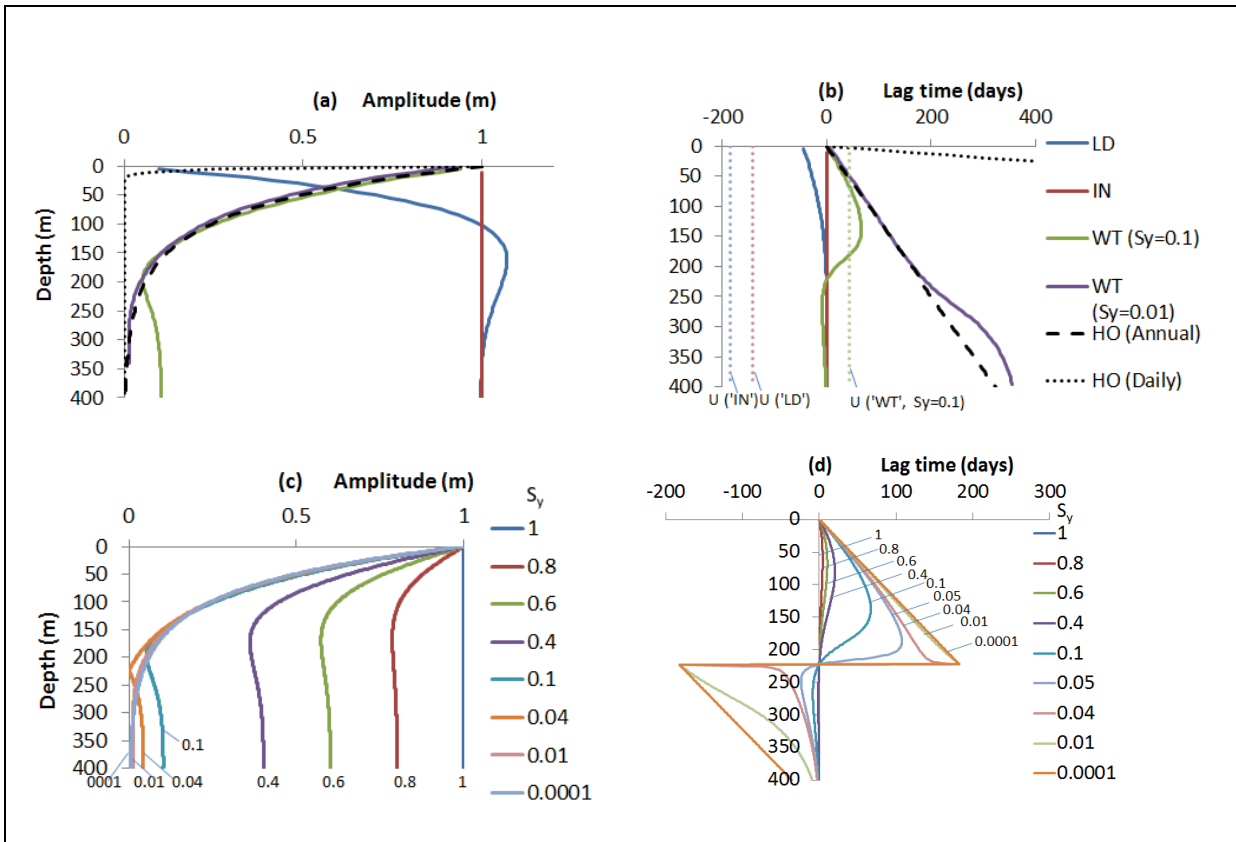
314 **3.1 The free surface water inundation scenario ('IN')**

315 Under free-surface water inundation, head changes are characteristically equal in amplitude at all depths and in-phase with the
316 inundation signal. Away from the top boundary, the instantaneous head due to loading in this case is $h = \xi L$. Since ξ is close
317 to 1 and $H = L$, the head is everywhere almost equal to the mechanical load given that at the top boundary the head is also
318 $h = H$. Therefore under free-surface water inundation in the absence of pumping, piezometers at all depths can be expected to
319 record the surface water mechanical load, effectively operating as weighing lysimeters. The vertical displacement of the ground
320 surface is extremely small (amplitude ~ 0.4 mm), being due to the small compression of porewater itself over the 1 km
321 simulated depth, and is out of phase with the load (i.e. the ground surface moves downwards under an increasing load). The
322 amplitude of change in saturated storage is infinitesimal (~ 0.02 mm). The system is essentially 'un-drained'; water does not
323 flow in or out of the pores which therefore experience only minimal strain.

324



325 Figure 4. 1D model simulations for the GBM environment, showing results for the scenarios (a) 'IN', (b) 'WT' ($S_y=0.1$), (c) 'WT'
 326 ($S_y=0.01$), (d) 'LD', (e) 'IN' with constant pumping, (f) 'IN' with cyclic pumping, (see text for explanation). The x-axis is time in
 327 days, shown to 10 years (i.e. 3650 days). The amplitudes reported in the text are calculated from the max-min of the last annual
 328 cycle. Left: The y-axis is head, in metres (m). The surface head and/or mechanical load boundary conditions (black line) are
 329 expressed as equivalent m head (for the WT condition the unit variation of head is given and the S_y variation in mechanical load is
 330 not shown); results are in green (30 m depth), blue (100 m depth) and red (300 m depth) in all cases. For (a) results are co-linear at
 331 all depths; for (f) the intermittent pumping is shown as off/on by the square-wave dotted line. Right: The y-axis has dimension of
 332 length, in metres (m), showing changes in storage (dashed red line) and surface displacement (solid blue line) for each scenario.



334 Figure 5. Profiles with depth for (a) amplitude of head response, (b) phase of head response and surface displacement (U), (c)
 335 sensitivity of amplitude to S_y for the 'WT' boundary condition, (d) sensitivity of phase to S_y for the 'WT' boundary condition. For
 336 (a) and (b) the colour code for the scenarios 'LD', 'IN', 'WT' ($S_y=0.1$), 'WT' ($S_y=0.01$), and HO, is shown in the top right panel (see
 337 text for explanation); in (b), displacement for the WT, $S_y=0.01$ scenario overlies that for the WT, $S_y=0.1$ scenario, so is not shown.

338 3.2 The variable water table scenario ('WT')

339 By contrast with the 'IN' scenario, head changes determined by a moving water table are depth-variable in amplitude and
 340 phase. When $S_y \rightarrow 0$ the 'WT' condition tends to the head-only end-member ('HO') and when $S_y \rightarrow 1$ the 'WT' condition
 341 tends to the 'IN' scenario. The maximum lag for $S_y = 0.1$ is at 137 m depth (or $\theta = 1.94$), beyond which it reduces (Fig. 5b).
 342 The sensitivity in head to S_y for the 'WT' scenario is illustrated in Fig. 5c. The amplitude of head responses is less than the
 343 water table fluctuation at all depths. Moreover, only a deep piezometer such as the one indicated at 300 m (Fig. 4b) will behave
 344 as a weighing lysimeter in this scenario. Here, heads are in phase with the water table and have approximate magnitude, $h =$
 345 $\xi L = \xi S_y H$, as in the study by (van der Kamp and Maathuis, 1991) of a thick aquitard overlying a confined aquifer. At 100 m
 346 the amplitude of head change is greater than at 300 m, and lags behind the water table. At 30 m the amplitude of head change
 347 is greatest and the lag is less than at 100 m. The difference in the head responses compared to the 'IN' scenario is due to the

348 difference in magnitudes of the applied head and applied load under the ‘WT’ scenario, causing an instantaneous internal head
349 gradient which subsequently diffuses. Ground surface displacement is ~4 mm and lags the load by 44 days. With increased
350 head at the top boundary, the upper surface moves upwards because as higher heads penetrate the aquifer the effective stress
351 is reduced. The lag is due to the time taken for the surface head to diffuse downwards.

352 3.3 The hydraulically disconnected load scenario (‘LD’)

353 Heads in the case of a surface load hydraulically isolated from the aquifer show a third characteristic behaviour. In this case
354 the amplitude of head change increases from zero at the top boundary (Fig. 5a), ~~and counter-intuitively reaches~~ reaching a
355 peak which is greater than the load, 1.07 m at 162 m (or $\theta = 2.29$). The amplitude thereafter tends to ξL at greater depth, whilst
356 the lag tends to zero. Therefore heads in relatively deep piezometers potentially represent the surface load under a ‘LD’
357 boundary condition, as in Fig. 4d where the heads at 300 m match the surface load, whereas at 30 m they do not. This is due
358 to upward head diffusion towards the surface where the head boundary condition is $h=0$. The lag which occurs in the ‘WT’
359 scenario due to the applied head exceeding the mechanical load is reversed in this ‘LD’ scenario, becoming a lead time as the
360 applied load exceeds the applied head. Surface displacement is out of phase with the load, leading by $\sim\pi$ radians. The ground
361 surface displacement amplitude of ~4 mm is ten times greater than for the ‘IN’ scenario but is still very small in comparison
362 to the annual variability of order 10 cm measured by GPS(Steckler et al., 2010). The ‘LD’ behaviour can be interpreted by
363 means of a decomposition of heads in the manner shown in (Anochikwa et al., 2012) (see Supporting Information).

364 3.4 The influence of pumping

365 Introduction of pumping from the depth interval 50-100 m causes hydraulic dis-equilibrium which continues well beyond the
366 ten years’ simulation, as the head drawdown propagates deep into the profile. As well as drawing water from storage at depth,
367 pumping induces recharge from the surface, there being a downward hydraulic gradient from the surface to the pumped
368 horizon, and upwards from the deeper levels to the pumped horizon. Variable perturbation due to the ‘IN’ surface load is
369 nevertheless clearly evident in the deep groundwater head measurements following correction for secular decline (Fig. 4e).
370 Elastic displacement, manifested as ground surface decline, exceeds 40 cm after ten years of pumping but, as in the un-pumped
371 ‘IN’ scenario, the annual fluctuation due to surface loading is vanishingly small (0.03 mm). Thus, in addition to the possibility
372 of irreversible plastic deformation, elastic strain may gradually increase due to continuous pumping as stored water is drawn
373 from increasing depths.

374

375 Intermittent pumping strongly increases the seasonal variation in heads at the depth of pumping and this disturbance diffuses
376 to adjacent levels. However, as in the case of continuous pumping, the surface load signal is largely preserved in the deep
377 groundwater head response at 300 m. Also, intermittent pumping induces the same average long-term secular decline in stored
378 water volume and ground surface displacement as continuous pumping, but with additional annual fluctuation caused by the

379 pump switching on and off (decline/drawdown during the dry period when the pumps are used for irrigation and recovery
380 during the rainy season when the pumps are off).

381 **3.5 Model results for ground surface displacement**

382 Taking into account a small correction for the compressibility of water, surface displacement in the model is almost equal to
383 the total change in elastic storage in the permanently saturated aquifer. For the cases where pumping dominates the removal
384 of water, surface displacement is in phase with the pumping (Fig. 4f). For the cases which set up a diffusion of the hydraulic
385 signal between the surface boundary and the aquifer, the phase of surface displacement depends on the hydraulic (non-loading)
386 head changes at all depths (Fig. 4b, c, d). Therefore the lag for vertical displacements under the 'LD' surface condition is $\sim\pi$
387 out of phase with displacement under the 'WT' condition. Note from Eq. [426] that the amplitude and lag are both a function
388 of $\theta = z \sqrt{\frac{\omega}{2D}} = z \sqrt{\frac{\pi}{DT}}$ and therefore the solutions given here would be scaled in z by any changes to bulk diffusivity, D , and
389 signal frequency (or time period, T): higher frequency would give the same distribution but for a smaller z and the reverse
390 would be true for diffusivity. Intermittent pumping produces the largest cyclic displacements, however, in the order of
391 centimetres, because this condition causes the greatest volume of seasonal drainage from the formation itself. Where there is
392 non-uniform loading, as produced for example by a variable river stage, lateral groundwater drainage may occur and surface
393 vertical displacements may be greater under these conditions too.

394

395 **4 Applying the partial coupling analysis to field data**

396 Applying the 1D partial-coupling analysis to field data, we examine poromechanical perturbations at two sites, Khulna and
397 Laksmipur in southern Bangladesh (Fig. 1). Hourly measurements of groundwater pressure made between April 2013 and June
398 2014 in three closely-spaced piezometers between 60 and 275 m depth at each site are illustrated as hydrographs of equivalent
399 freshwater head in Supporting Information. The objective here is to apply the principles and assumptions of the partially-
400 coupled hydro-mechanical approach to reproduce the characteristic features of the multi-level groundwater hydrographs using
401 broadly representative aquifer parameters, rather than to attempt an exact match by inverse modelling. Inspection of the
402 hydrographs at both sites indicates, by reference to Figures 4 and 5, that mechanical loading significantly influences the
403 measured heads. Additionally, the presence of thick clay aquitards at both sites (Figures 6, 7) suggests conditions under which
404 heads may be determined solely by mechanical loads and piezometers might behave as geological weighing lysimeters; a
405 possibility which we put to the test.

406

407 The approach at each site is as follows:

- 408 i. A two-component sand-clay stratigraphy is based on site data, and parameter values are selected from the ranges described
409 in Section 2.
- 410 ii. The piezometric readings are compared to examine possible pumping influences which need to be taken into account in the
411 model by means of a simple abstraction pattern. Based on what is known about nearby abstractions an appropriate pumping
412 depth interval is determined. The magnitude of the extraction rate is manually adjusted as a fitting parameter.
- 413 iii. Where a piezometer is uninfluenced by pumping we test its behaviour as a geological weighing lysimeter. The heads in the
414 chosen piezometer are assumed to define the mechanical load at the surface, and this assumption is tested for self-consistency
415 by comparison of the simulations to the data from all three piezometers.
- 416 iv. The nature of the upper head boundary is then examined by reference to the implications for a variety of hydraulic loading
417 conditions. For a 'WT' boundary, changing S_y manually as a fitting parameter adjusts the magnitude of the applied heads
418 concomitant with the mechanical load.

419 **4.1 Groundwater levels at Khulna, south-west Bangladesh**

420 At Khulna town(Burgess et al., 2014) piezometers KhPZ60, KhPZ164 and KhP271 (the numbers indicate depth to the
421 piezometer screen in metres) are located 700 m from the ~300 m wide tidal Rupsa River, in a grassy compound which also
422 contains municipal water-supply pumping boreholes (Supporting Information). The lithological sequence (Fig. 6) comprises a
423 surface clay layer overlying sand in which KhPZ60 is screened, and a deeper layer of clay at 100 m separating the shallow
424 sand from a deeper sand formation in which KhPZ164 and KhPZ271 are screened. Year-round pumping from 250-300 m depth
425 maintains a consistent downward head difference of ~3 m between the uppermost and the lower two piezometers. It is the
426 transient head variations rather than the absolute steady-state head differences that are of interest here. Bodies of standing
427 water in the vicinity, water in the unsaturated zone, and shallow groundwater combine with the sinuous Rupsa River as sources
428 of TWS load; groundwater pumping is an additional source of hydraulic variation.

429

430 The three Khulna hydrographs are characterised by periodic variations containing tidal frequency components throughout the
431 rising and falling limb of the annual cycle, and a series of episodic increments superimposed on the rising limb during the
432 monsoon season; the annual amplitude of groundwater head variation is ~2.5 m. Amplitude of the tidal frequency components
433 increases between 60 m and 164 to 271 m depth, with no phase lag and with a consistent synchronicity between the piezometer
434 heads and the Rupsa River water level fluctuations including the semi-diurnal and spring-neap cycles (Fig. 6 and Supporting
435 Information). Episodic deflections on the hydrograph rising limbs, coincident with rainfall events, are likewise simultaneous
436 at all measurement depths (Burgess et al., 2014). Therefore by reference to the partial coupling analysis (Figures 4 and 5) it is
437 evident that heads in the Khulna piezometers respond primarily to mechanical loading by a combination of monsoon water
438 and tidal loading.

439

440 At a daily level the time series of groundwater heads in KhPZ164 and KhPZ271 include an additional frequency component
441 which simple analysis of head differences confirms as the hydraulic influence of the daily municipal pumping schedule from
442 which KhPZ60 is protected by an intermediate clay layer. Therefore KhPZ60 alone is taken as recording a solely mechanical
443 loading response and the KhPZ60 head record is applied as the upper boundary condition to represent the varying TWS load
444 at the surface in a 1D hydro-mechanical model of the Khulna site (Fig. 6), assuming $\beta=1$. The upper boundary resolves all
445 sources of load acting at the site including from the Rupsa River, which is a linear rather than an areally-extensive load. The
446 ratio of daily variability in head at KhPZ60 and in the Rupsa River level is ~ 0.06 , therefore the 1.23 m annual variation in river
447 stage would explain ~ 0.07 m head variation in KhPZ60, only 3% of the total. Therefore 97% of the annual variation in head
448 at KhPZ60 is attributable to changes in TWS other than load transmitted from the river, representing areally-extensive loads
449 as required by the 1D partially-coupled analysis. Given the relatively well-drained urban context at Khulna and the absence of
450 areally-extensive open water that otherwise characterises the rural areas of the GBM floodplains, a 'WT' condition is most
451 likely the dominant loading style, but other sources of loading may also contribute. The layered structure of the Khulna model
452 (Fig. 6) has clay at 0-50 m and 100-150 m with sand in between. The daily municipal pumping cycle is implemented as a
453 source term of 2.4 m a^{-1} for 12 hours of each day applied over the interval 200 to 350 m, the rate having been manually adjusted
454 by reference to the daily head fluctuations in KhPZ164 and KhPZ271.

455
456
457
458
459
460
461
462
463
464
465
466
467
468
469
470

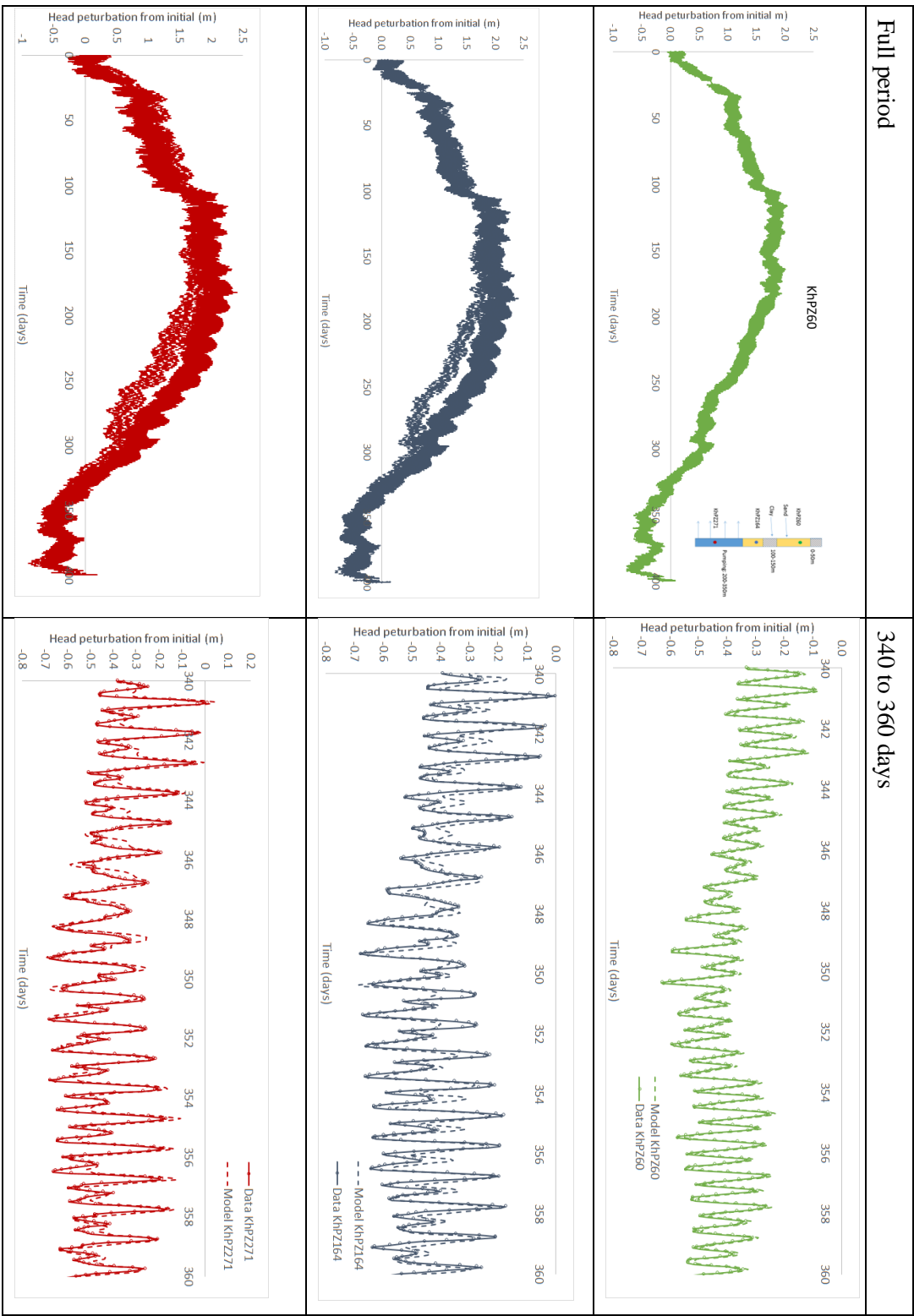


Figure 6. Knuha: comparison of observed heads (solid lines) and simulated heads (dashed lines), starting 27 April 2013, for WT upper boundary condition ($S_2=0.4$). X-axis is time in days. The surface loading is set equal to the observed head in KhPZ60 divided by S_2 . The pumping rate is $2.4 \text{ m}^3 \text{ a}^{-1}$ for 12 hours of each day, switching on at 05:45 am. Top (green) is KhPZ60, middle (blue) is KhPZ164, bottom (red) is KhPZ271.

471

472 Figure 6 compares the measured groundwater heads with the heads simulated by the model under the assumption of a ‘WT’
 473 boundary with S_y assigned a value of 0.4, with $\kappa_{sand} = 1 \times 10^{-5} \text{ m s}^{-1}$, $\kappa_{clay} = 1 \times 10^{-9} \text{ m s}^{-1}$, $S_S = 10^{-4} \text{ m}^{-1}$ (corresponding to
 474 $E = 82.07 \text{ MPa}$), $\nu = 0.25$ and $n = 0.1$. The results are insensitive to S_y being varied in the range from 0.1 to 1 (the latter being
 475 equivalent to an ‘IN’ boundary), and are near-identical in the case of a ‘LD’ boundary (Supporting Information). This is
 476 because the upper clay effectively isolates the piezometers from the surface hydraulically.

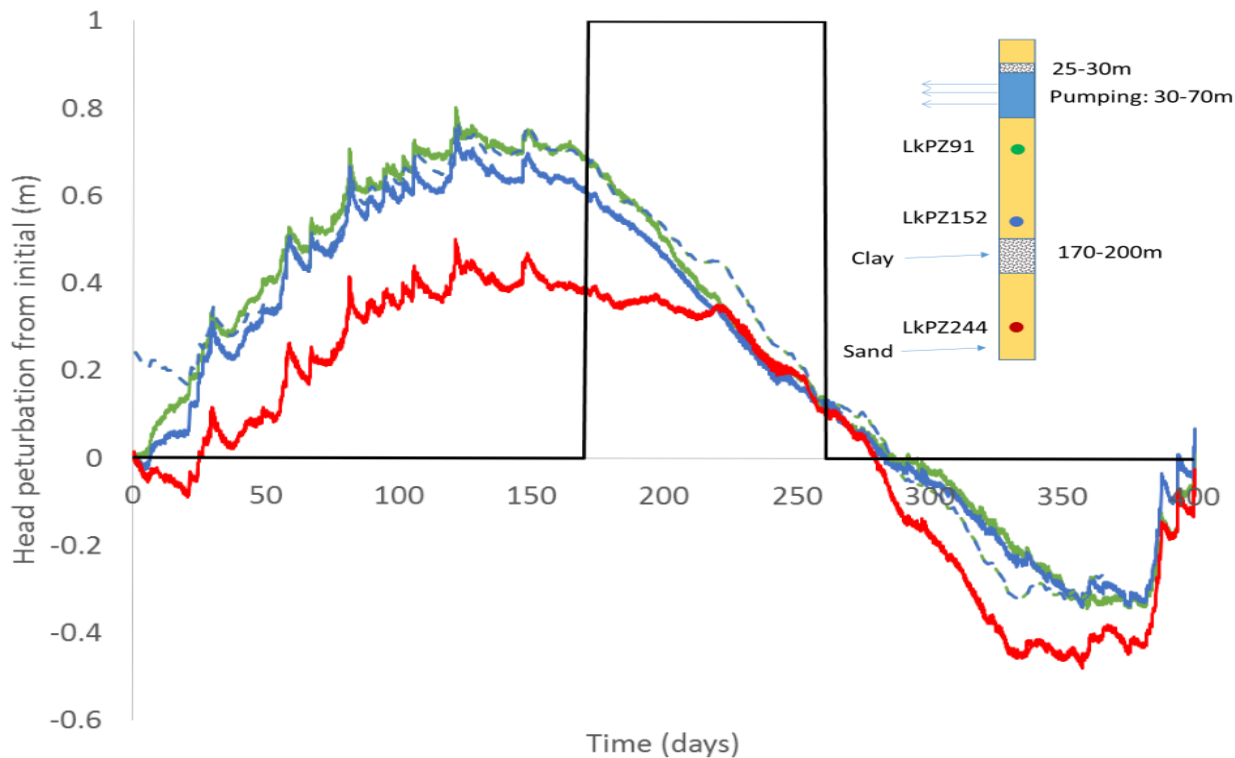
477 4.2 Groundwater levels at Laksmipur, south-west-east Bangladesh

478 At Laksmipur (Burgess et al., 2017) the piezometers LkPZ91, LkPZ152 and LkPZ244 are situated in a rural region of rice-
 479 paddy and tree plantations on the Lower Meghna floodplain (Supporting Information), 10 km distant from the River Meghna
 480 and 8 km from municipal boreholes which pump from 270–300 m depth. Seasonal pumping from depths up to 100 m for rice
 481 irrigation is common in the vicinity. The lithological sequence indicates fine sand with occasional silty clay layers. The
 482 hydrographs are characterised by a sequence of episodic increments in groundwater head associated with periods of heavy
 483 rainfall producing a rising limb of amplitude $\sim 1 \text{ m}$ through the monsoon season; during the dry-season recession, minor
 484 periodic fluctuations of order 0.01 m containing atmospheric frequency components become more clearly evident (Burgess et
 485 al., 2017). The episodic increments are almost synchronous and of consistent magnitude at all piezometer depths, indicative
 486 by reference to Figures 4 and 5 of groundwater heads responding dominantly to mechanical loading and unloading due to
 487 changes in TWS above the aquifer surface.

488

489 Here, cyclical head differences between LkPZ244 and the shallower two piezometers indicate hydraulic influences of dry-
 490 season pumping on the LkPZ91 and LkPZ152 hydrographs, whereas downward propagation of the hydraulic signals to
 491 LkPZ244 is prevented by the clay layer between 170 and 200 m depth. Therefore LkPZ244 is taken as recording a solely
 492 mechanical loading response and the LkPZ244 head record is applied as the upper boundary condition to represent the varying
 493 TWS load at the surface in a 1D hydro-mechanical model of the Laksmipur site (Fig. 7). with a small offset applied to the
 494 initial heads above 170 m depth, consistent with the observed head perturbations being shown as starting from a common zero
 495 value. All styles of upper boundary were applied (‘IN’, ‘LD’, and ‘WT’ with a range of S_y values, see Supporting Information)
 496 in an attempt to distinguish the dominant source of TWS load around the site from the boundary style leading to the best fit
 497 with piezometer measurements. In all other respects the models incorporate the dimensions and assumptions as described in
 498 Sect. 3, with sand ($\kappa_{sand} = 1 \times 10^{-5} \text{ m s}^{-1}$) and three-two clay layers (BWDB, 2013) at 25–30 m, 115–130 m and 170–200 m (κ_{clay}
 499 $= 1 \times 10^{-8} \text{ m s}^{-1}$), and $E = 82.07 \text{ MPa}$. A simple dry-season pumping regime over a 105 day period starting 17 November 2013 is
 500 implemented as a source term of 0.04 m a^{-1} applied over the interval 30 to 70 m in the model, manually adjusted by reference
 501 to the LkPZ91 and LkPZ152 hydrographs.

502



503

504 **Figure 7. Laksmipur: comparison of observed heads (solid lines) and simulated heads (dashed lines) starting 31 May 2013, for ‘WT’**
 505 **upper boundary condition ($S_y=0.8$), for LkPZ91 (green), LkPZ152 (blue) and LkPZ244 (red). X axis is time in days. The surface**
 506 **loading is set equal to the observed head in LkPZ244, and the surface head is set to the observed head in LkPZ244 divided by S_y .**
 507 **The pumping rate is 0.04 m a^{-1} for the period shown (1 for ‘on’, 0 for ‘off’).**

508

509 For LkPZ244 the simulated heads are an excellent match with measurements over the entire period. The simulated heads for
 510 the shallower two piezometers LkPZ91 and LkPZ152 most closely match the measurements under a ‘WT’ boundary with S_y
 511 assigned a value of 0.8 (Fig. 7 and [Supporting Information](#)). ~~The consistently higher simulated heads compared to~~
 512 ~~observations at LkPZ152 could be simply explained by the sands at that depth having a lower loading efficiency.~~ The model
 513 results therefore confirm that LkPZ244 is isolated from the hydraulic effects of water table variation and of seasonal pumping,
 514 and the LkPZ244 groundwater head variation over the observation period is determined solely by mechanical loads at the
 515 surface. Therefore LkPZ244 is validated as acting effectively as a geological weighing lysimeter (Burgess et al., 2017).

516

517 For the shallower piezometers, the best fit value for S_y is higher than is reasonable for fine sand and more likely indicates the
 518 combined effects of a variable water table and fluctuating levels of standing water, in drainage channels and on paddy fields
 519 around the piezometer site, consistent with the field situation. As a consequence of seasonal pumping at 0.04 m a^{-1} , the model
 520 shows groundwater is both drawn from storage and induced as recharge from the upper surface, but the amplitude of saturated

521 storage fluctuation is only 6 mm, therefore changes to the water budget are dominated by recharge to the water-table. The
522 surface displacement is predicted at 6 mm amplitude, in phase with the changes in storage.

523 **5 Discussion**

524 **5.1 Aquifer responses to discrete modes of terrestrial water variation**

525 Models based on the 1D partially-coupled hydro-mechanical analysis confirm that substantial poroelastic influences should be
526 expected in the Bengal Aquifer System, and that groundwater heads respond characteristically to changes in specific terrestrial
527 water stores (Figures 4 and 5). Only laterally-extensive flooding above an aquifer fully saturated to the ground surface (the
528 'IN' loading style) will drive instantaneous and synchronous head variations at all depths determined by the loading efficiency,
529 inducing negligible flow of groundwater. In any situation involving a variable water table (the 'WT' loading style) and for any
530 variable loads hydraulically disconnected from the aquifer (the 'LD' style), hydraulic gradients are imposed due to the unequal
531 magnitude of stress and head at the surface. These gradients take time to dissipate, depending on the frequency of the signal
532 fluctuation and the aquifer hydraulic diffusivity, and so lead to differences in amplitude and phase of the head response with
533 depth. In these situations, the relative importance of the hydraulic and mechanical influence is controlled by the aquifer
534 hydraulic diffusivity, the loading efficiency and the depth of interest. In the case of a fluctuating water table, the difference
535 between the head and stress signals is a function of the specific yield, S_y , in the zone of fluctuation.

536

537 The characteristic responses of the aquifer might therefore provide a key to identifying the terrestrial water store dominating
538 Δ TWS, by monitoring vertical profiles of groundwater head. Multiple terrestrial water stores will normally contribute,
539 however, as at Laksmipur and Khulna, so a unique identification may not be possible. This limitation is inherent to the 1D
540 analysis, which resolves all the contributions to load into one upper boundary condition respectively for head and stress. The
541 analysis indicates how different loads and dynamic responses superpose to produce the observed groundwater hydrographs. In
542 principle, key aspects of the water balance may be better estimated by de-convolving known components of the Δ TWS signal.
543 (Anochikwa et al., 2012) [assembled field measurements of rainfall and evapotranspiration at a site in Saskatchewan, Canada,](#)
544 [using them to define the upper boundary conditions in a one-dimensional model to examine their hydraulic and mechanical](#)
545 [loading separately, before summing the outcomes to simulate the overall hydro-mechanical influence on groundwater pressure.](#)
546 [Having determined loading efficiency by reference to barometric effects, they then calibrated their 1D model against observed](#)
547 [groundwater pressures by varying hydraulic conductivity.](#) At Khulna and Laksmipur, [measurements of the separate](#)
548 [components of the terrestrial water cycle were not available, hence an indirect demonstration of hydro-mechanical effects was](#)
549 [desirable, the The 1D partially-coupled analysis leads to good agreement between simulated and observed heads are in good](#)
550 [agreement,](#) consistent with the local conditions, [so confirming the 1D partially-coupled analysis](#) as a suitable basis for
551 representing the poroelastic behaviour of the BAS.

552 5.2 Significance for groundwater monitoring and geological weighing lysimetry

553 In terms of the extent to which piezometer water levels indicate recharge and drainage, it is only where there is a rapid hydraulic
554 connection between the piezometer and the water table that the piezometer will be sensitive to head change at the water table
555 and therefore to changes in unconfined storage. If a piezometer is hydraulically isolated from surface water and/or the water
556 table and is beyond other transient hydraulic influences, it can respond to changes in the weight of the TWS load, acting as a
557 geological weighing lysimeter (van der Kamp and Maathuis, 1991; Smith et al., 2017). In this case, where the changing load
558 is due to a moving water table, knowledge of the loading efficiency allows the load measurement to be converted into an
559 estimate of recharge and discharge.

560

561 In all other situations, a wide range of coupled hydro-mechanical responses can be expected, as we have shown for the BAS
562 (Figures 4 and 5). Seasonally-variable groundwater heads (Fig. 4) are therefore open to misinterpretation as seasonally-variable
563 groundwater storage, leading to error in determination of recharge if the poroelastic nature of the response is neglected.
564 Consider heads at 30 m, a common depth for Bangladesh Water Development Board (BWDB) monitoring boreholes
565 (Shamsudduha et al., 2011). For the case of a variable load hydraulically disconnected from the aquifer (Fig. 4d) the annual
566 water level rise is equal to half the amplitude of the load yet augmentation of elastic storage, by definition in this case, is nil.
567 For the case of variable TWS inundation (Fig. 4a) the annual groundwater level rise is equivalent to the annual depth of
568 inundation yet augmentation of elastic and unconfined storage is insignificant. Conversely, relative to a variable water table
569 (Fig. 4b,c) groundwater fluctuation at 30 m depth is attenuated. Failure to account for this would lead to an underestimate of
570 recharge to unconfined storage by about 30%. The error increases as hydraulic diffusivity decreases, therefore errors could be
571 expected to be greater in the coastal regions of the Bengal Basin where the thickness of silty-clays is greater (Mukherjee et al.,
572 2007). Considerable caution is therefore necessary in the use of even relatively shallow piezometers as indicators of recharge
573 to the water table. A true indication of recharge requires either a shallow tubewell screened over the depth interval of actual
574 water table fluctuation, or a deep piezometer responding as a geological weighing lysimeter to the varying mass provided by
575 a fluctuating water table. In the latter case it is recharge to the shallow water table that is measured, not recharge at the depth
576 of the piezometer.

577

578 The 1D hydro-mechanical framework can be applied as a test for the special cases where groundwater head responds solely to
579 mechanical load, and hence to validate the use of geological weighing lysimetry. The laterally-extensive loading criterion
580 inherent to the 1D analysis must apply, and the piezometer screen must be isolated or distant from hydraulic transients
581 originating at the surface or from pumping. We have shown for the BAS that these requirements most likely occur at depths
582 beyond about 250 m, as in the case of 'WT' and 'LD' loading styles in the absence of pumping (Fig. 5). The inundation ('IN')
583 style of TWS variation leads to instantaneous transmission of head without loss of amplitude at all depths; in this case
584 piezometers at all depths provide a mechanical record of Δ TWS rather than a hydraulic record of storage variation and to infer

585 recharge would lead to 100% error. Our analysis demonstrates a solely mechanical loading response at 244 m depth at
586 Laksmipur, below the level of seasonal irrigation pumping, and at 60 m depth at Khulna, above the level of deep pumping for
587 municipal water supply.

588 **5.3 Significance for ground surface displacements and groundwater storage changes**

589 The models also demonstrate the amplitude and phase of ground surface displacement as a hydro-mechanical consequence of
590 varying terrestrial water stores, and the significance of pumping (Fig. 4e and 4f). Under simplifications associated with the 1D
591 model, vertical surface displacements relative to a fixed model base at 1 km depth are approximately equal to the change in
592 elastic storage, the small difference being due to compressibility of water. These changes are minor in the BAS under all TWS
593 loading styles, in the order of mm, compared to the displacements in the case of seasonal groundwater pumping which are in
594 the order of cm. Seasonal surface displacements in the order of cm have also been attributed to strain acting over a depth scale
595 of hundreds of kilometres due to the load applied by monsoonal inundation over the entire Bengal Basin (Steckler et al., 2010).
596 Strains due to seasonal groundwater pumping at shallow depths may therefore be in the same order of magnitude but out of
597 phase with crustal strain, making ground surface deflections a poor proxy for changing elastic storage in the aquifer. As a
598 corollary, interpretation of seasonal ground surface fluctuations across the GBM floodplains solely in terms of deep crustal
599 deformation(Steckler et al., 2010) potentially requires reassessment in the light of BAS aquifer poroelasticity.

600 **5.4 Limitations and further consequences**

601 In our analysis we have based values for the 3D loading efficiency, β (0.961-0.996) and Young's Modulus, E (82-851 MPa)
602 in the BAS on field measurements of S_s , for the sake of internal hydro-mechanical consistency, but we have noted a discrepancy
603 with lower values for the 1D loading efficiency ξ (0.69-0.87) derived from determinations of barometric efficiency(Burgess
604 et al., 2017). These differences require attention, but the overall conclusions on the significance of poroelastic behaviour in
605 the BAS and the pattern of poroelastic responses characteristic of specific upper surface TWS boundary conditions are
606 unaffected. [Although we omitted barometric effects in the generic simulations for the sake of simplicity, it is straightforward](#)
607 [to superpose a further loading signal on top of the existing one if required, as for example when deconvolving deep piezometric](#)
608 [signals to make water resources assessments](#) (Anochikwa et al., 2012).

609
610 Under certain circumstances the extensive load assumption inherent in the 1D analysis may break down. Rivers, as linear
611 sources of head and load, can be accommodated within the 1D framework where their contribution to the TWS load is minor
612 as demonstrated at Khulna. In general however, rivers should be expected to impose laterally variable heads and require a
613 more generalised 2D or 3D fully-coupled poro-mechanical treatment(Boutt, 2010;Pacheco and Fallico, 2015). An equivalent
614 constraint applies to strains, an additional reason for surface displacement not to offer a secure proxy for groundwater storage
615 in the BAS. The dense distribution of rivers, distributaries and drainage channels in the Bengal Basin makes the BAS widely

616 vulnerable to loading effects that may not adequately be reduced to a 1D description; 13% and 47% of 1035 piezometers in
 617 the BWDB groundwater monitoring network lie within 1 and 5 km respectively of a river.

618 **6 Conclusions**

619 We argue that a 1D *partially-coupled* approach to hydro-mechanical processes, whereby the loading term is included in the
 620 flow equation without the need to simultaneously compute the elastic equation, is a suitable basis for representing the
 621 poroelastic behaviour of the Bengal Aquifer System when surface conditions can be treated as areally extensive. Applying a
 622 1D *partially-coupled* hydro-mechanical analysis we have shown how the BAS responds characteristically to specific sources
 623 of terrestrial water storage variation. Rivers can be incorporated as a component of the 1D load where their contribution is
 624 small, but in general will require a 2D or fully 3D treatment.

625
 626 Groundwater levels, groundwater recharge, vertical groundwater flow and ground surface elevations are all influenced by the
 627 poroelastic behaviour of the BAS. Our results expose the error of the conventional assumption of de-coupled hydraulic
 628 behaviour which underlies previous assessments of recharge to the BAS. Also they demonstrate the complexities in applying
 629 ground surface displacements as a proxy measure for variations in groundwater storage. We propose that the 1D *partially-*
 630 *coupled* analysis can be applied to validate when geological weighing lysimetry is applicable in the BAS. In some situations,
 631 geological weighing lysimetry offers an alternative approach to recharge assessment.

633 Appendix: Poromechanical equations

634 The constitutive isotropic relation between elastic stress and strain, coupled to the pore-pressure by Terzaghi's effective stress
 635 law is given by (Neuzil, 2003):

$$\sigma_{ij} = 2G\varepsilon_{ij}\delta_{ij} + 2G\frac{\nu}{1-2\nu}\varepsilon_{kk}\delta_{ij} + \alpha_B p\delta_{ij} \quad (A1)$$

636 where δ_{ij} is the Kronecker delta (which is zero when $i \neq j$ and one when $i = j$) and following the Einstein Summation
 637 convention; stresses (σ_{ij}) and strains (ε_{ij}) are positive in compression; p is the porewater pressure (Pa), ν is Poisson's ratio (-
 638), G is the shear modulus (MPa), and $\alpha_B = 1 - K/K_s$, where, K (MPa) is the bulk modulus of the porous medium and K_s
 639 (MPa) is the bulk modulus of the solid grains.

640
 641 Just as the elastic equations have a pore pressure term, the isothermal, Darcian groundwater flow equation contains a coupled
 642 stress term (Neuzil, 2003):

$$\nabla \cdot \kappa(\nabla p + \rho g \nabla z) = S_{s3} \frac{\partial p}{\partial t} - S_{s3} \beta \frac{\partial \sigma_t}{\partial t} - gJ \quad (A2)$$

643 where κ is the hydraulic conductivity (m s^{-1}), p is the pore pressure (Pa), z is the elevation (m), J is a source term used here
 644 to simulate groundwater abstraction by pumping and $\sigma_t = (\sigma_{xx} + \sigma_{yy} + \sigma_{zz})/3$ (Pa).

645

646 The 3D specific storage is defined as:

$$S_{s3} = \rho g \left[\left(\frac{1}{K} - \frac{1}{K_s} \right) + \left(\frac{n}{K_f} - \frac{n}{K_s} \right) \right] \quad (\text{A3})$$

where n is the porosity, and K_f is the modulus of the water (MPa).

The (3D) loading efficiency, or Skempton's coefficient, β , is defined as:

$$\beta = \frac{\left(\frac{1}{K} - \frac{1}{K_s} \right)}{\left(\frac{1}{K} - \frac{1}{K_s} \right) + \left(\frac{n}{K_f} - \frac{n}{K_s} \right)} \quad (\text{A4})$$

647

648 **Author contributions**

649 WGB conceived the study; NDW led the mathematical analysis and the numerical modelling; all authors contributed to the
 650 scenario descriptions and consideration of the modelling results; NDW and WGB drafted the manuscript; all authors reviewed
 651 the manuscript.

652

653 **Acknowledgments**

654 We acknowledge funding from the UK EPSRC Global Challenges Research Fund (UCL/BEAMS EPSRC GCRF award
 655 172313) to WGB for research on *Poroelasticity in the Bengal Aquifer System and groundwater resources monitoring in*
 656 *Bangladesh*. NDW thanks the University of Southampton for leave of absence during the course of the project. Field
 657 measurements at Khulna and Laksmipur were made with the kind assistance of the Bangladesh Water Development Board
 658 (BWDB) and financial support from the UK Department for International Development (DfID) under the project *Groundwater*
 659 *Resources in the Indo-Gangetic Basin* (Grant 202125-108) managed by Professor Alan MacDonald of the British Geological
 660 Survey. We are grateful to Professors Mike Steckler, Columbia University, and Humayun Akhter, Dhaka University, for useful
 661 discussions on ground surface vertical motions in the Bengal Basin, and to John Barker and William Powrie for helpful
 662 discussion of the fundamental processes at the start of the research. Dr. Mohammed Shamsudduha, University College
 663 London, and Ms. Sarmin Sultana, Dhaka University are thanked for discussions on the hydrological context of the groundwater
 664 level monitoring piezometers. The data used are listed in the references and illustrated in the Supporting Information.

665 **Nomenclature**

666	α	Proportion of mechanical load as head
667	α_B	Biot-Willis coefficient, $1 - K/K_s$
668	β, C	3D loading efficiency, Skempton's coefficient, or 'tidal efficiency'
669	δ_{ij}	Kronecker delta
670	ε_{ij}	Strain
671	θ	$z \sqrt{\frac{\omega}{2D}} = z \sqrt{\frac{\pi}{DT}}$
672	λ	$2\alpha_B(1 - 2\nu)/3(1 - \nu)$
673	ν	Poisson's ratio
674	ξ	1D loading efficiency
675	κ	Hydraulic conductivity
676	ρ	Water density
677	σ_{ij}	Stress tensor
678	σ_t	Total stress
679	ψ	Lag (radians)
680	ω	Angular frequency
681		
682	a	River half-width
683	B	Barometric efficiency
684	E	Young's Modulus
685	D	Hydraulic diffusivity
686	g	Acceleration due to gravity
687	G	Shear Modulus
688	h	Head
689	$H(t)$	Top boundary head
690	H_0	Amplitude of top boundary head
691	J	Fluid source term
692	K	Bulk Modulus of porous medium
693	K_f	Bulk modulus of the water
694	K_s	Bulk modulus of the solid grains
695	$L(t)$	Top boundary load
696	L_0	Amplitude of top boundary load

697	n	Porosity
698	p	Pore pressure
699	S_y	Specific Yield
700	S_s	Specific storage
701	S_{s3}	3D Specific storage
702	t	Time
703	u	Vertical displacement
704	x	Perpendicular distance from a river
705	z	Vertical coordinate
706		

707 **References**

708

709 COMSOL Multiphysics® v. 5.2. www.comsol.com. . COMSOL AB, Stockholm, Sweden.

710 Acworth, R. I., Rau, G. C., McCallum, A. M., Andersen, M. S., and Cuthbert, M. O.: Understanding connected surface-

711 water/groundwater systems using Fourier analysis of daily and sub-daily head fluctuations, Hydrogeology Journal, 23, 143-

712 159, 10.1007/s10040-014-1182-5, 2015.

713 Anochikwa, C. I., van der Kamp, G., and Barbour, S. L.: Interpreting pore-water pressure changes induced by water table

714 fluctuations and mechanical loading due to soil moisture changes, Canadian Geotechnical Journal, 49, 357-366, 2012.

715 Bakker, M.: The effect of loading efficiency on the groundwater response to water level changes in shallow lakes and

716 streams, Water Resources Research, 52, 1075-1715, doi:10.1002/2015WR017977, 2016.

717 Bardsley, W. E., and Campbell, D. J.: A new method for measuring near-surface moisture budgets in hydrological systems,

718 Journal of Hydrology, 154, 245-254, 1994.

719 Bardsley, W. E., and Campbell, D. J.: Natural geological weighing lysimeters: calibration tools for satellite and ground

720 surface gravity monitoring of subsurface water-mass change, Natural Resources Research, 9, 147-156, 2000.

721 Bardsley, W. E., and Campbell, D. J.: An expression for land surface water storage monitoring using a two-formation

722 geological weighing lysimeter, Journal of Hydrology, 335, 240-246, 2007.

723 Barr, A. G., van der Kamp, G., Schmidt, R., and Black, T. A.: Monitoring the moisture balance of a boreal aspen forest using

724 a deep groundwater piezometer, Agricultural and Forest Meteorology, 102, 13-24, 2000.

725 Benner, S. G., Polizzotto, M. L., Kocar, B. D., Ganguly, S., Phan, K., Ouch, K., Sampson, M., and Fendorf, S.: Groundwater

726 flow in an arsenic-contaminated aquifer, Mekong Delta, Cambodia, Applied Geochemistry, 23, 3072-3087, 2008.

727 Bense, V. F., and Person, M. A.: Transient hydrodynamics within intercratonic sedimentary basins during glacial cycles,

728 Journal of Geophysical Research:Earth Surface (2003-2012), 113, 2008.

729 Black, J. H., and Barker, J. A.: The puzzle of high heads beneath the West Cumbrian coast, UK: a possible solution,

730 Hydrogeology Journal, 24, 439-457, 10.1007/s10040-015-1340-4 2016.

731 Boutt, D. F.: Poroelastic loading of an aquifer due to upstream dam releases, Ground Water, 48, 580-592, 2010.

732 Burbey, T. J., Warner, S. M., Blewitt, G., Bell, J. W., and Hill, E.: Three-dimensional deformation and strain induced by

733 municipal pumping, part 1: Analysis of field data, Journal of Hydrology, 319, 123-142, 2006.

734 Burgess, W. G., Hoque, M. A., Michael, H. A., Voss, C. I., Breit, G. N., and Ahmed, K. M.: Vulnerability of deep

735 groundwater in the Bengal Aquifer System to contamination by arsenic, Nature Geoscience, 3, 83-87, 10.1038/ngeo750,

736 2010.

Burgess, W. G., Shamsudduha, M., Taylor, R. G., Zahid, A., Ahmed, K. M., Mukherjee, A., and Lapworth, D. J.: Seasonal, episodic and periodic changes in terrestrial water storage recorded by deep piezometric monitoring in the Ganges/Brahmaputra/Meghna delta, AGU Fall Meeting 2014, San Francisco, 2014.

Burgess, W. G., Shamsudduha, M., Taylor, R. G., Zahid, A., Ahmed, K. M., Mukherjee, A., Lapworth, D. J., and Bense, V. F.: Terrestrial water load and groundwater fluctuation in the Bengal Basin, *Scientific Reports*, 7(1), 3872, 10.1038/s41598-017-04159-w, 2017.

BWDB: Establishment of monitoring network and mathematical model study to assess salinity intrusion in groundwater in the coastal area of Bangladesh due to climate change. Final report. , Bangladesh Water Development Board, Dhaka, 773, 2013.

Chaussard, E., Burgmann, R., Shirzaei, M., Fielding, E. J., and Baker, B.: Predictability of hydraulic head changes and characterization of aquifer-system and fault properties from InSAR-derived ground deformation, *Journal of Geophysical Research: Solid Earth*, 119, 6572–6590, 10.1002/2014JB011266, 2014.

de Silva, S., Wightman, N. R., and Kamruzzaman, M.: Geotechnical ground investigation for the Padma Main Bridge, IABSE-JSCE Joint Conference on Advances in Bridge Engineering-II, Dhaka, Bangladesh, 2010,

Domenico, P. A., and Schwartz, F. W.: *Physical and Chemical Hydrogeology*, 2nd ed., John Wiley & Sons, New York, 1998.

Erban, L. E., Gorelick, S. M., and Zebker, H. A.: Groundwater extraction, land subsidence, and sea-level rise in the Mekong Delta, Vietnam, *Environmental Research Letters*, 9, 10.1088/1748-9326/9/8/084010, 2014.

Fendorf, S., Michael, H. A., and van Geen, A.: Spatial and temporal variations of groundwater arsenic in south and southeast Asia, *Science*, 328, 1123-1127, 2010.

Gibson, R. E.: The analytical method in soil mechanics, *Geotechnique*, 24, 115-140, 1974.

Green, D. H., and Wang, H. F.: Specific storage and poroelastic coefficient, *Water Resources Research*, 26, 1631-1637, 1990.

Hasanuzzaman, S. M.: Impact of groundwater utilisation on agriculture, in: *Groundwater resources and development in Bangladesh: background to the arsenic crisis, agricultural development and the environment*, edited by: Rahman, A. A., and Ravenscroft, P., Bangladesh Centre for Advanced Studies, University Press Ltd., Dhaka, 161-185, 2003.

Hoque, M. A., Burgess, W. G., and Ahmed, K. M.: Integration of aquifer geology, groundwater flow and arsenic distribution in deltaic aquifers – A unifying concept, *Hydrological Processes*, 31, 2095-2109, <https://doi.org/10.1002/hyp.11181>, 2017.

Hussain, M. M., and Abdullah, S. K. M.: Geological setting of the areas of arsenic safe aquifers. Report of the ground water task force, Ministry of Local Government, Rural Development & Cooperatives, Local Government Division, Bangladesh Interim Report No. 1, 2001.

Jacob, C. E.: On the flow of water in an elastic artesian aquifer, *Transactions of the American Geophysical Union*, 574-586, 1940.

Lambert, A., Huang, J., van der Kamp, G., Henton, J., Mazzotti, S., James, T. S., Courtier, N., and Barr, A. G.: Measuring water accumulation rates using GRACE data in areas experiencing glacial isostatic adjustment: The Nelson River basin, *Geophysical Research Letters*, 40, 6118-6122, 10.1002/2013GL057973, 2013.

Larsen, F., Pham, N. Q., Dang, N. D., Postma, D., Jessen, S., Pham, V. H., Nguyen, T. B., Trieu, H. D., Tran, L. T., Nguyen, H., Chambon, J., Nguyen, H. V., Ha, D. H., Hue, N. T., Duc, M. T., and Refsgaard, J. C.: Controlling geological and hydrogeological processes in an arsenic contaminated aquifer on the Red River flood plain, Vietnam, *Applied Geochemistry*, 23, 3099-3115, 2008.

Manga, M. I., Beresnev, I., Brodsky, E. E., Elkhoury, J. E., Elsworth, D., Ingebritsen, S. E., Mays, D. C., and Wang, C.-Y.: Changes in permeability caused by transient stresses: field observations, experiments, and mechanisms, *Reviews of Geophysics*, 50, 10.1029/2011RG000382, 2012.

Marin, S., van der Kamp, G., Pietroniro, A., Davison, B., and Toth, B.: Use of geological weighing lysimeters to calibrate a distributed hydrological model for the simulation of land-atmosphere moisture exchange, *Journal of Hydrology*, 383, 179-185, 2010.

Michael, H. A., and Voss, C. I.: Evaluation of the sustainability of deep groundwater as an arsenic-safe resource in the Bengal Basin, *PNAS*, 105, 8531-8536, 2008.

Michael, H. A., and Voss, C. I.: Estimation of regional-scale groundwater flow properties in the Bengal Basin of India and Bangladesh, *Hydrogeology Journal*, 17, 1329-1346, 10.1007/s10040-009-0443-1, 2009a.

787 Michael, H. A., and Voss, C. I.: Controls on groundwater flow in the Bengal Basin of India and Bangladesh: regional
788 modeling analysis, *Hydrogeology Journal*, 17, 1561-1577, 10.1007/s10040-008-0429-4, 2009b.

789 Mukherjee, A., Fryar, A. E., and Rowe, H. D.: Regional hydrostratigraphy and groundwater flow modeling of the arsenic
790 affected western Bengal basin, West Bengal, India, *Hydrogeology Journal*, 15, 1397-1418, 10.1007/s10040-007-0208-7,
791 2007.

792 Narasimhan, T. N.: On storage coefficient and vertical strain, *Ground Water*, 44, 488-491, 2006.

793 Neuzil, C. E.: Hydromechanical coupling in geological processes, *Hydrogeology Journal*, 11, 41-83, 2003.

794 Pacheco, F. A. L., and Fallico, C.: Hydraulic head response of a confined aquifer influenced by river stage fluctuations and
795 mechanical loading, *Journal of Hydrology*, 531, 716-727, <http://dx.doi.org/10.1016/j.jhydrol.2015.10.055>, 2015.

796 Powrie, W.: *Soil Mechanics: Concepts and Applications*, 3rd ed., CRC Press, Taylor and Francis Group, Boca Raton,
797 Florida, 2014.

798 Rahman, M. A. T., Majumder, R. K., Rahman, S. H., and Halim, M. A.: Sources of deep groundwater salinity in the
799 southwestern zone of Bangladesh, *Environmental Earth Sciences*, 63, 363-373, 2011.

800 Ravenscroft, P.: Overview of the hydrogeology of Bangladesh, in: *Groundwater resources and development in Bangladesh:*
801 *background to the arsenic crisis, agricultural potential and the environment*, edited by: Rahman, A. A., and Ravenscroft, P.,
802 Bangladesh Centre for Advanced Studies, University Press Ltd., Dhaka, 43-86, 2003.

803 Ravenscroft, P., Burgess, W. G., Ahmed, K. M., Burren, M., and Perrin, J.: Arsenic in groundwater of the Bengal Basin,
804 Bangladesh: Distribution, field relations, and hydrogeological setting, *Hydrogeology Journal*, 13, 727-751, 10.1007/s10040-
805 003-0314-0, 2005.

806 Ravenscroft, P., Brammer, H., and Richards, K. S.: *Arsenic pollution: a global synthesis*, First ed., Wiley-Blackwell, UK,
807 616 pp., 2009.

808 Ravenscroft, P., McArthur, J. M., and Hoque, M. A.: Stable groundwater quality in deep aquifers of Southern Bangladesh:
809 The case against sustainable abstraction, *Sci Total Environ.*, 454-455, 627-638, 2013.

810 Reeves, J. A., Knight, R., Zebker, H. A., Kitanidis, P. K., and Schreuder, W. A.: Estimating temporal changes in hydraulic
811 head using InSAR data in the San Luis Valley, Colorado, *Water Resources Research*, 50, 4459-4473,
812 10.1002/2013WR014938, 2014.

813 Roeloffs, E. A.: Fault stability changes induced beneath a reservoir with cyclic variations in water level, *Journal of*
814 *Geophysical Research*, 93, 2107-2124, 1988.

815 Rojstaczer, S., and Agnew, D. C.: The influence of formation material properties on the response of water levels in wells to
816 Earth tides and atmospheric loading, *Journal of Geophysical Research*, 94, 12,403-412,411, 1989.

817 Shamsudduha, M., Taylor, R. G., Chandler, R. E., and Ahmed, K. M.: Basin-scale variations in shallow groundwater levels
818 in Bangladesh over the last 40 years: assessing the impacts of groundwater-fed irrigation. In: *Water scarcity and water*
819 *security seminar*, Geological Society, London, U. K., 2008.

820 Shamsudduha, M., Taylor, R. G., Ahmed, K. M., and Zahid, A.: The impact of intensive groundwater abstraction on
821 recharge to a shallow regional aquifer system: evidence from Bangladesh, *Hydrogeology Journal*, 19, 901-916,
822 10.1007/s10040-011-0723-4, 2011.

823 Shamsudduha, M., Taylor, R. G., and Longuevergne, L.: Monitoring groundwater storage changes in the highly seasonal
824 humid tropics: validation of GRACE measurements in the Bengal Basin, *Water Resour. Res.*, W02508,
825 10.1029/2011WR010993, 2012.

826 Shamsudduha, M., Zahid, A., and Burgess, W. G.: Security of deep groundwater against arsenic contamination in the Bengal
827 Aquifer System: a numerical modelling study in southest Bangladesh, *Sustainable Water Resources Management*
828 doi.org/10.1007/s40899-018-0275-z, 2018.

829 Smith, C., van der Kamp, G., Arnold, L., and Schmidt, R.: Measuring precipitation with a geolysimeter, *Hydology and Earth*
830 *System Science*, 21, 5263-5272, 2017.

831 Spane, F. A.: Considering barometric pressure in groundwater flow investigations, *Water Resources Research*, 38,
832 10.1029/2001WR000701, 2002.

833 Steckler, M. S., Noonan, S. L., Akhter, S. H., Chowdhury, S. K., Bettadpur, S., Seeber, L., and Kogan, M. G.: Modeling earth
834 deformation from monsoonal flooding in Bangladesh using hydrographic, GPS and GRACE Data, *Journal of Geophysical*
835 *Research*, 115, 10.1029/2009JB007018, 2010.

836 Sultana, S., Ahmed, K. M., Mahtab-Ul-Alam, S. M., Hasan, M., Tuinhof, A., Ghosh, S. K., Rahman, M. S., Ravenscroft, P.,
837 and Zheng, Y.: Low-cost aquifer storage and recovery: implications for improving drinking water access for rural
838 communities in coastal Bangladesh, *Journal of Hydrologic Engineering*, 20, B5014007-5014001-5014012,
839 10.1061/(ASCE)HE.1943-5584.0001100., 2015.

840 Sutherland, R., Townend, J., Toy, V., Upton, P., Coussens, J., Allen, M., and etc.: Extreme hydrothermal conditions at an
841 active plate-bounding fault, *Nature*, 546, 137-140, 10.1038/nature22355, 2017.

842 Tam, V. T., Batelaan, O. L. T. T., and Nhan, P. Q.: Three-dimensional hydrostratigraphical modelling to support evaluation
843 of recharge and saltwater intrusion in a coastal groundwater system in Vietnam, *Hydrogeology Journal*, 22, 1749-1762,
844 2014.

845 Tapley, B. D., Bettadpur, S., Ries, J. C., Thompson, P. F., and Watkins, M. M.: GRACE measurements of mass variability in
846 the Earth system, *Science*, 305, 503-505, 2004.

847 Tiwari, V. M., Wahr, J., and Swenson, S.: Dwindling groundwater resources in northern India, from satellite gravity
848 observations, *Geophys. Res. Lett.*, 36, L18401, 10.1029/2009GL039401, 2009.

849 van der Kamp, G., and Gale, J. E.: Theory of Earth tide and barometric effects in porous formations with compressible
850 grains, *Water Resources Research*, 19, 538-544, 1983.

851 van der Kamp, G., and Maathuis, H.: Annual fluctuations of groundwater levels as a result of loading by surface moisture,
852 *Journal of Hydrology*, 127, 137-152, 1991.

853 van der Kamp, G., and Schmidt, R.: Monitoring of total soil moisture on a scale of hectares using groundwater peizometers,
854 *Geophysical Research Letters*, 24, 719-722, 1997.

855 van der Kamp, G., and Schmidt, R.: Review: Moisture loading - the hidden information in groundwater observation well
856 records, *Hydrogeology Journal*, 25, 2225-2233, 10.1007/s10040-017-1631-z, 2017.

857 Verruijt, A.: Elastic storage of aquifers, in: *Flow through porous media*, edited by: Weist, R. J. M. d., Academic Press Inc.,
858 New York, 331-376, 1969.

859 Xu, X., Huang, G., Qu, Z., and Pereira, L. S.: Using MODFLOW and GIS to assess changes in groundwater dynamics in
860 response to water saving measures in irrigation districts of the Upper Yellow River Basin, *Water Resources Management*,
861 25, 2035-2059, 2011.

862

863